

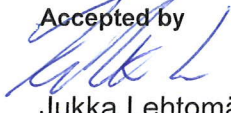


Characterisation of the produced particles by the IndMeas industrial flow calibration device – filter collection experiments with active tracer particles

Authors: Jussi Lyyränen¹, Ville Laukkanen², Aleksi Ahola² and Ari Auvinen¹
1 VTT, P.O. Box 1000, FI-02044 VTT, Finland,
2 IndMeas, Tietäjantie 12, FI-02130 ESPOO, Finland

Confidentiality: Confidential

Report's title	
Characterisation of the produced particles by the IndMeas industrial flow calibration device – filter collection experiments with active tracer particles	
Customer, contact person, address	Order reference
Ville Laukkanen IndMeas, Tietäjäsentie 12, FI-02130, Espoo, Finland	
Project name	Project number/Short name
SHOK CLEEN/MMEA/2010-15/SONE E	71091-1.2
Author(s)	Pages
Jussi Lyyränen, Ville Laukkanen, Aleksi Ahola and Ari Auvinen	28
Keywords	Report identification code
Particle measurement, tracer particle, flow calibration, filter	VTT-R-04832-14
Summary	
<p>In this study the produced particles (TiO_2, $\text{Fe}(\text{NO}_3)_2 \cdot 9\text{H}_2\text{O}$, BaCl_2 and $\text{Ni}(\text{NO}_3)_2$) by the IndMeas flow calibrator device (FCD) directly enter the measurement system (continuous production) or the particles were collected on the surface of a new filter and removed by a fast and powerful "blow" similar as in the case of the cyclone (filter collection). In addition to the earlier experiments the concentration of the feed solutions is further varied and active ^{137}Ba-tracer is applied as in the normal field measurements. To study the effect of higher temperature on the size of the tracer particles an additional heater ($T=150^\circ\text{C}$; of the same order as temperature at the exit of the FCD) was installed after flow calibration device before the collection filter. Moreover, to simulate possible particle adhesion and retention in systems containing moisture near or at the inlet point of the tracer particle feed a so called "wet inlet tube" experiment was carried out. Finally, possible particle adhesion and retention caused by a non-optimal inlet tube was studied by installing a long spiral-type inlet tube.</p> <p>The change of reagent concentration did change the number of produced particles but their size remained basically unchanged ($d_p \geq 1 \mu\text{m}$). Lowering the reagent concentration even more would not probably be of any use because collection times (to attain high enough activation level of the particles) would also need to be increased thus increasing the probability for agglomeration on the filter.</p> <p>The addition of an additional heater clearly improved the collection of particles on the filter by decreasing thermophoretic losses. The addition of a wet inlet tube to simulate possible particle adhesion in systems containing moisture near or at the inlet point of the tracer particle was found effective in trapping the particles: up to 2.5-fold decrease in number concentration was found. Another, even more efficient particle trap was an addition of a long spiral inlet tube to simulate non-optimal inlet tube causing particle adhesion and retention: up to 20-fold decrease in number concentration was found. Thus selecting an optimal inlet and inlet tube is very important to minimise particle losses.</p> <p>The reentrainment of the particles from the filter during the pressure "blow" may be improved by selecting another filter material that is less porous. The main problem in finding a suitable filter material is that it has to withstand the high pressure peak reentraining the particles during the "blow". One solution could be a dense metal grid or sintered metal filter. These types of filters withstand pressure peaks, and the detachment or reentrainment of the collected particles should be easier.</p>	
Confidentiality	{Public, Restricted, Confidential}
Espoo 22.10.2014	
Written by	Reviewed by
	
Jussi Lyyränen Senior Scientist (Dr. Sc.)	Ari Auvinen Research Team Leader
Accepted by	
	
Jukka Lehtomäki Research Team Leader	
VTT's contact address	
P.O. Box 1000, FI-02044 VTT, Finland	
Distribution (customer and VTT)	
{Customer, VTT and other distribution. In confidential reports the company, person and amount of copies must be named. Continue to next page when necessary.}	
<p><i>The use of the name of the VTT Technical Research Centre of Finland (VTT) in advertising or publication in part of this report is only permissible with written authorisation from the VTT Technical Research Centre of Finland.</i></p>	

Contents

Contents.....	2
1. Introduction.....	3
2. Methods.....	4
2.1 Principles of measurement devices.....	4
2.2 Studied process and measurement set-up.....	4
2.3 Experimental matrix.....	6
3. Results and discussion	7
3.1 Filter collection and continuous production of particles for TiO ₂ , Fe(NO ₃) ₂ ·9H ₂ O and BaCl ₂ with and without silica	7
3.1.1 Particle number concentration and number size distribution	7
3.1.2 Particle morphology	8
3.2 Filter collection of particles with heater for TiO ₂ , Fe(NO ₃) ₂ ·9H ₂ O, BaCl ₂ and Ni (NO ₃) ₂ with and without silica	12
3.2.1 Particle number concentration and number size distribution	12
3.2.2 Particle morphology	14
3.3 Filter collection of particles with heater and with wet inlet tube for TiO ₂ , Fe(NO ₃) ₂ ·9H ₂ O and BaCl ₂ with and without silica.....	17
3.3.1 Particle number concentration and number size distribution	17
3.3.2 Particle morphology	18
3.4 Filter collection of particles with heater and with spiral inlet tube for TiO ₂ , Fe(NO ₃) ₂ ·9H ₂ O and BaCl ₂ with and without silica.....	22
3.4.1 Particle number concentration and number size distribution	22
3.4.2 Particle morphology	23
4. Summary and conclusions.....	25
References.....	28

1. Introduction

This study titled as “Production and dispersion of tracer particles for process flow measurements” is a part of the CLEEN MMEA (Measurement, monitoring and environmental efficiency assessment) research program going on during 2010-2014. The aim of the research program is “to combine the development of new measurement technologies, data quality assurance methods, modelling and forecasting tools, and information and communication technology (ICT) infrastructure (CLEEN MMEA factsheet, 2010).”

A measurement (calibration) device designed by the IndMeas company for the calibration of industrial flow meters with the help of activated particles is studied and characterised. With this device it is also possible to check/evaluate, e.g. emissions and energy balances of an industrial facility. The method applies ^{137}Ba -tracer, whose $t_{d,1/2}=153$ s. The aim of the research is to characterise the IndMeas measurement method and to improve its performance. The main focus is to concentrate on thoroughly charactering the particles produced by the device with different reagents, and on improving the properties of the particles, i.e. to reduce their adherence and decrease their size to reduce particle losses by, e.g. deposition.

2. Methods

2.1 Principles of measurement devices

In the following section a short description of the experimental techniques and equipment used in this study is provided. For more thorough information the required references are provided.

An aspiration electron microscopy sampler (AEM sampler) was used to collect samples for morphology studies in scanning electron microscope (SEM). The sampler consists of an EM grid mounting head soldered with silver into 6 mm tubing and Swagelok fittings. The carbon coated copper grid (Holey carbon, $d_{\text{grid}}=3.1 \text{ mm}$) is mounted on the grid mounting head with the help of a hollow screw, and a copper seal is mounted between the screw and the EM grid. The flow through the aspiration sampler is regulated to approximately 0.1 Nlpm with a critical orifice (CO). This sampler is designed and manufactured by VTT.

An electrical low-pressure impactor (ELPI) was used to measure the particle number concentration and number size distribution. The base of the ELPI is a 12 stage cascade low-pressure impactor with a without a final filter stage. In these measurements the ELPI is equipped with a filter stage. In ELPI the particles are charged with a unipolar diode charger to a well-defined charge level prior entering the cascade impactor. Inside the impactor the particles are classified in to 12 size classes (from 30 nm to 10 μm) according to their aerodynamic diameter. When collected at the different collection stages the particles produce electric current that is measured with highly sensitive electrometers. The results may then be recorded to a PC equipped with a control software (Keskinen, et al., 1992; Baltensperger, Weingartner, Burtscher and Keskinen, 2001).

2.2 Studied process and measurement set-up

The operation principles of IndMeas flow calibrator device (FCD) is described in the research report (Lyyränen, et al., 2011). In this study the cyclone used for the collection of the produced particles is replaced by a filter (Fig. 1a). The collected particles are removed from the surface of the filter by a fast and powerful pressure pulse, "blow", similar as in the case of the cyclone. This process is called filter collection.



Figure 1a Measurement set-up for filter collection experiments with active tracer particles.



Figure 1b. Sample line for measuring tracer particles "blown" from the filter.

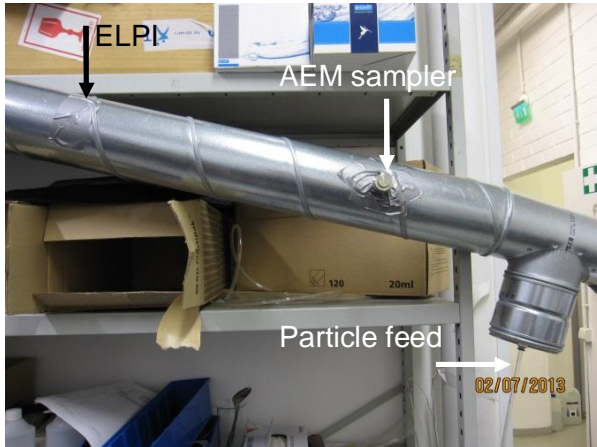


Figure 1c. Sample inlet locations for AEM microscopy sampler and ELPI.

In the previous experiments particle number and mass concentration and number size distribution has been characterised in detail (Lyyränen, et al., 2011; Lyyränen, et al., 2012). In these experiments similar reagents are used to produce the particles as in previous experiments with the exception that the concentration of the feed solutions is further varied and active ^{137}Ba -tracer is applied. The tracer particles are used to study the collection efficiency of the filter and re-entrainment of the collected particles by the pressure “blow” by measuring the signal intensity generated by the particles as in the field measurements. The signal generated by the activated tracer particles was monitored by radiation detectors at the FCD exit, at the filter and outside the sampling tube near sampling point. To find out the size of the generated tracer particles samples for scanning electron microscopy are collected with the AEM microscopy sampler. In addition, to monitor the re-entrainment of the particles after the “blow” particle number concentration and size distribution are measured with an ELPI. Moreover, to find out the possible size difference between the particles collected on the filter that are “blown” away (**filter collection**) and the particles produced by the FCD before filter collection, microscopy samples were collected directly from the outlet of the flow calibrator device without the filter (**continuous production**). During this collection no ELPI measurement was carried out. Comparison of these particle samples indicates possible agglomeration/aggregation of the particles during filter collection.

To study the effect of higher temperature on the size of the tracer particles an additional heater ($T=150\text{ }^{\circ}\text{C}$; of the same order as temperature at the exit of the FCD) was installed after flow calibration device before the collection filter (Fig. 1a). The function of the heater is to ensure that the particles arriving to the filter are completely moisture free that may cause unwanted aggregation/adherence of particles to each other. Moreover, to simulate possible particle adhesion and retention in systems containing moisture near or at the inlet point of the tracer particle feed a so called “wet inlet tube” experiment was carried out. Finally, possible particle adhesion and retention caused by a non-optimal inlet tube was studied by installing a long spiral-type inlet tube.

The sampling line (Fig. 1b) in these experiments is different from the previous ones: the line does not have any dilution and the tracer particle inlet is in right angle in relation to the sampling line (Fig. 1c). This is not optimal for minimising particle losses at the tracer particle inlet but in field measurements this is the most common case. Therefore, this type of particle inlet was selected. In the laboratory conditions the particle inlet could have been optimised by a 90 degree inlet probe extending parallel in to the sampling line. However, the probe was not used because the application of the probe in the field measurements is seldom possible.

2.3 Experimental matrix

The experimental matrix is presented in Table 1. The selected reagents were TiO₂, TiO₂ + silica, Fe(NO₃)₃·9H₂O, Fe(NO₃)₃·9H₂O+silica, Ni(NO₃)₂ + silica and BaCl₂ in different concentrations. The eluent solution passing through the activated ion exchange column was 0.005 mol/dm³ HCl solution in all cases. As in earlier studies, BaCl₂ acted as reference reagent.

Table 1. Measurement matrix for the experiments. Used reagents, processes (filter collection or continuous production (no filter)) and electron microscopy sample collection times. Reagent concentration and feed rate are also given (no filter = particle collection directly from the flow calibrator device without filter collection; heater = additional heater installed at the exit of the FCD before filter collection; wet inlet tube = to simulate possible particle adhesion and retention in systems containing moisture near or at the inlet point).

Date	Reagent(s)	Time	Process	SEM
1.7.2013	TiO ₂ + silica 20 g/dm ³ , 6 ml/min	10:20-10:37	Filter	10:37
		11:08-11:25		11:13
	TiO ₂ + silica 20 g/dm ³ , 6 ml/min	11:50-12:20	No filter	12:05
	Fe(NO ₃) ₃ ·9H ₂ O+Si 40 g/dm ³ , 6 ml/min	12:38-12:43		12:42
	BaCl ₂ 5.5 g/dm ³ , 6 ml/min	12:50-13:00		12:53
2.7.2013	TiO ₂ + silica 20 g/dm ³ , 3 ml/min	9:00-9:10	No filter	9:03
	TiO ₂ + silica 10 g/dm ³ , 3 ml/min	9:12-9:20		9:15
	Fe(NO ₃) ₃ ·9H ₂ O 2 g/dm ³ , 6 ml/min	9:22-9:30		9:27
	Background	9:32-9:40		9:35
	Fe(NO ₃) ₃ ·9H ₂ O 2 g/dm ³ , 6 ml/min	9:50-10:00	Filter	Low activity on filter
	TiO ₂ + silica 20 g/dm ³ , 6 ml/min	10:10-10:18		Particles adhere on filter
	TiO ₂ + silica 20 g/dm ³ , 6 ml/min	11:00-11:13	Filter + heater	11:07
	TiO ₂ + silica 20 g/dm ³ , 3 ml/min Fe(NO ₃) ₃ ·9H ₂ O 2 g/dm ³ , 6 ml/min	11:23-11:30 11:43-12:00		11:30 Low activity on filter
3.7. 2013	Fe(NO ₃) ₃ ·9H ₂ O+Si 40 g/dm ³ , 6 ml/min	9:20-9:30	Filter + heater	9:28
	BaCl ₂ 5.5 g/dm ³ , 6 ml/min	9:41-9:50		9:49
	BaCl ₂ 5.5 g/dm ³ , 6 ml/min	10:14-10:20	Filter + heater + wet inlet tube	10:18
	Fe(NO ₃) ₃ ·9H ₂ O+Si 40 g/dm ³ , 6 ml/min	10:27-10:36		10:35
	TiO ₂ + silica 20 g/dm ³ , 6 ml/min	10:53-11:03		11:02
	Fe(NO ₃) ₃ ·9H ₂ O+Si 40 g/dm ³ , 6 ml/min	11:10-11:15		11:15

	TiO ₂ + silica 20 g/dm ³ , 3 ml/min	11:30-11:40		11:38
	Fe(NO ₃) ₃ ·9H ₂ O 2 g/dm ³ , 6 ml/min	11:45-11:55		11:51
4.7.2013	Fe(NO ₃) ₃ ·9H ₂ O 2 g/dm ³ , 6 ml/min	9:40-9:50	Filter + heater + spiral	9:45
	TiO ₂ + silica 10 g/dm ³ , 6 ml/min	9:55-10:05		10:00
	TiO ₂ + silica 20 g/dm ³ , 6 ml/min	10:15-10:22		10:21
	Fe(NO ₃) ₃ ·9H ₂ O+Si 40 g/dm ³ , 6 ml/min	10:30-10:40		10:37
	BaCl ₂ 5.5 g/dm ³ , 6 ml/min	10:45-10:55		10:52
	Ni(NO ₃) ₂ 2 g/dm ³ , 6 ml/min	11:00-11:10	Filter + heater	11:09
	Ni(NO ₃) ₂ + silica 20 g/dm ³ , 6 ml/min	11:15-11:22		11:21
	Ni(NO ₃) ₂ + silica 2 g/dm ³ , 6 ml/min	11:24-11:27		

3. Results and discussion

3.1 Filter collection and continuous production of particles for TiO₂, Fe(NO₃)₂·9H₂O and BaCl₂ with and without silica

3.1.1 Particle number concentration and number size distribution

Typical particle number concentration during the **filter collection** with **TiO₂ + silica reagent** (20 g/dm³, 6 ml/min) for the first set on 1.7. at 10:20-10:37 varied between 2.8-3.8·10⁶ 1/cm³ and the aerodynamic count median diameter (CMD_{ae}) of the particles varied from 2 to 6 μm (Fig. 2a). A SEM sample was also collected. For the second set at 11:08-11:25 the number concentration varied between 0.7-1.7·10⁶ 1/cm³ and the CMD_{ae} varied from 1 to 2 μm. In addition, the CMD_{ae} of the escaped particles was larger than target size of approximately 0.5 μm. For the third set on 2.7. at 10:10-10:18 the number 1.6-5.7·10⁶ 1/cm³ and the CMD_{ae} was approximately 1 μm (Fig. 2b).

The number concentrations seemed to be slightly low thus indicating that only part of the particles was able to escape from the filter during the “blow”. Thus particles adhered to the filter. Another cause for a low total number concentration would be thermophoretic losses after the particles exit the flow calibrator device: The exit line leading to the filter is not usually insulated or heated.

For **Fe(NO₃)₃·9H₂O reagent** (2 g/dm³, 6 ml/min) during **filter collection** the particle number concentration on 2.7. at 9:50-10:00 varied between 1.4-3.6·10⁶ 1/cm³ and the CMD_{ae} varied from 0.1 to 0.3 μm (Fig. 2b). The CMD_{ae} in this case was optimal but the activity of the collected particles on the filter was low. Therefore, no SEM sample collection was considered necessary.

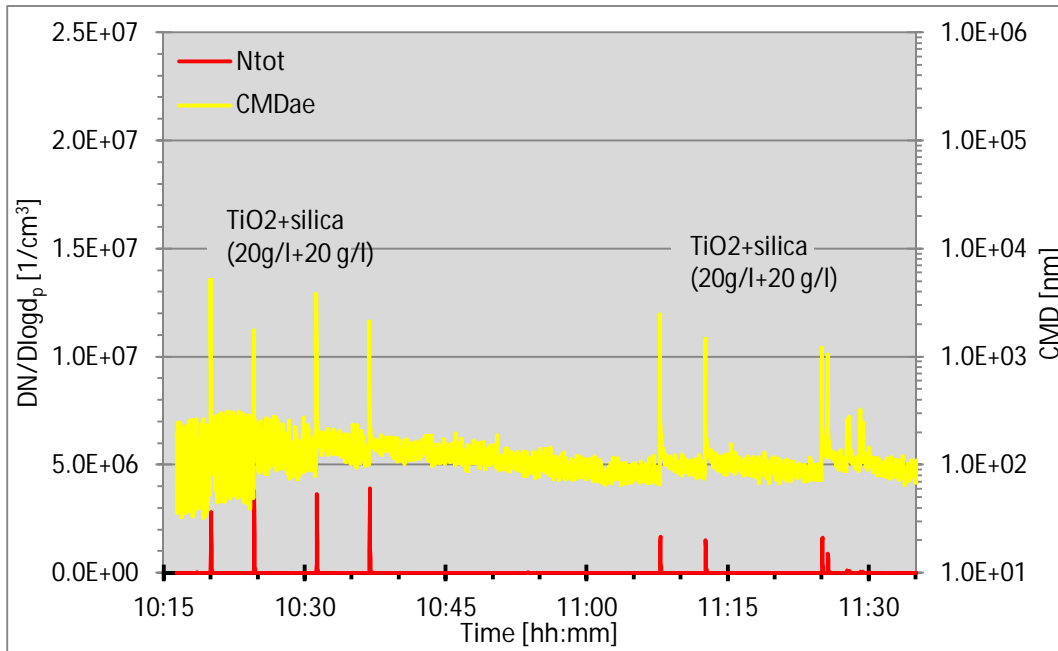


Figure 2a. Total particle number concentration and aerodynamic count median diameter (CMD_{ae}) of the particles generated from TiO_2 + silica reagent measured with ELPI on 1.7. 2013, filter collection.

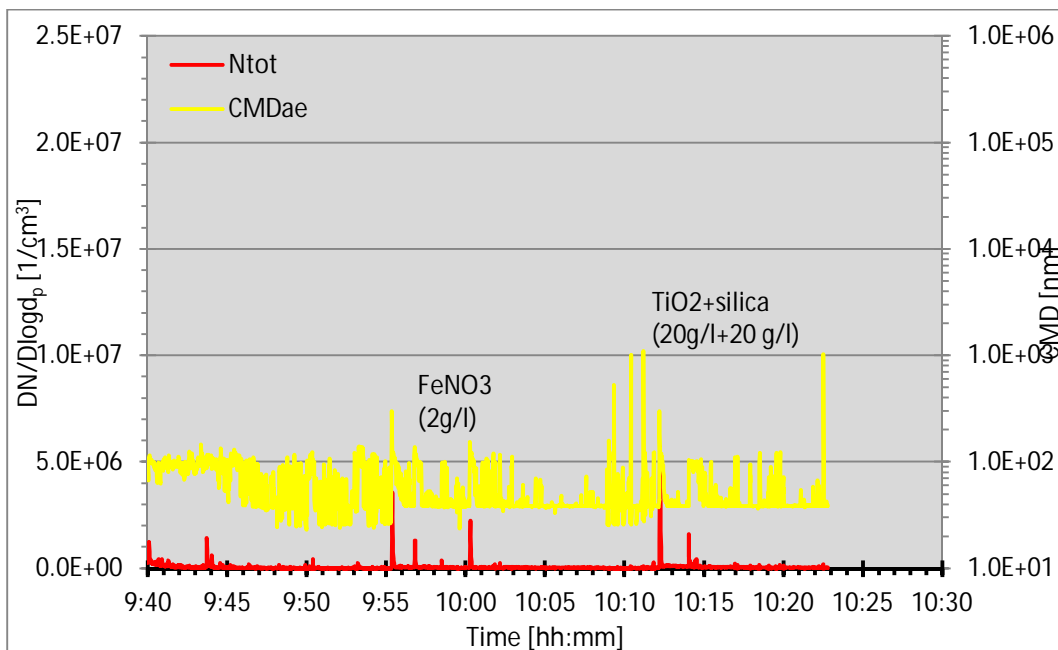


Figure 2b. Total particle number concentration and aerodynamic count median diameter (CMD_{ae}) of the particles generated from $Fe(NO_3)_3 \cdot 9H_2O$ and TiO_2 + silica reagent measured with ELPI on 2.7. 2013, filter collection.

3.1.2 Particle morphology

The produced particles with **TiO_2 + silica reagent** (20 g/dm^3 , 6 ml/min) **with filter collection** on 1.7. at 10:37 were mainly chain-like aggregates. The length of the aggregates varied a lot from a few hundred nanometres up to micrometres. This is in congruent with the CMD_{ae} measured with ELPI. The aggregates consisted of nearly spherical primary particles of approximately 50 nm in size (Fig. 3).

The produced particles with **TiO₂ + silica reagent** (20 g/dm³, 6 ml/min) **with continuous production** on 1.7. at 2013, 12:05 were spheres generally larger than 1 μm in diameter. The large spheres consisted of nearly spherical primary particles of approximately 50 nm in size (Fig. 4) as in the case of filter collection (Fig. 3).

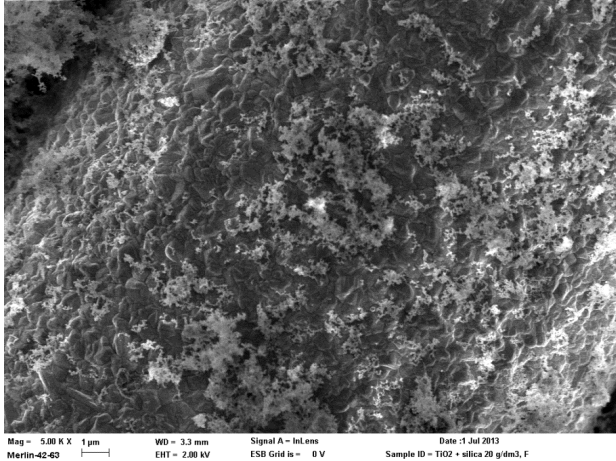


Figure 3a. The generated particles with TiO₂ + silica (20 g/dm³, 6 ml/min) reagent with filter collection (1.7.2013, 10:37). Particles are chain-like aggregates.

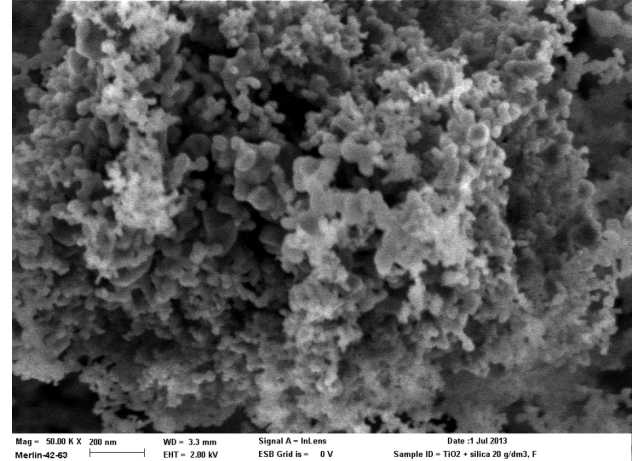


Figure 3b. A detailed image of the aggregates. They consist of spherical primary particles of approximately 50 nm in diameter.

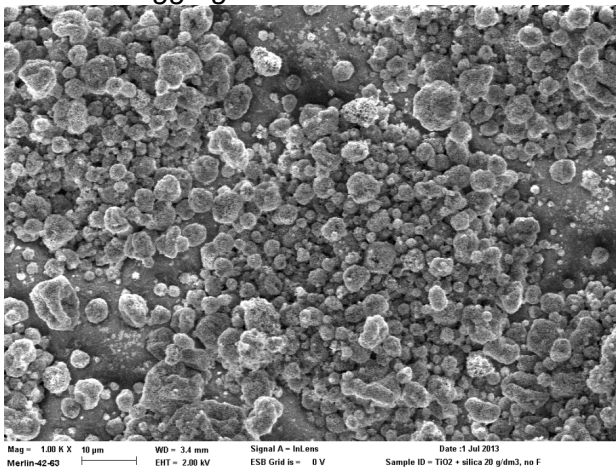


Figure 4a. The generated particles with TiO₂ + silica (20 g/dm³, 6 ml/min) reagent with continuous production (1.7.2013, 12:05). Particles are spheres generally larger than 1 μm in diameter.

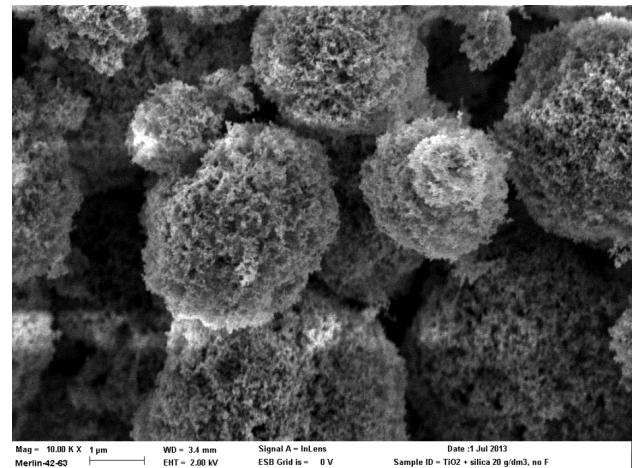


Figure 4b. A detailed image of the spheres. They consist of spherical primary particles of approximately 50 nm in diameter.

Comparison of SEM images for TiO₂ + silica reagent (20 g/dm³, 6 ml/min) with filter collection and continuous production indicated that the large spheres seen during continuous production (Fig. 4) seemed to disintegrate into smaller chain-like aggregates with filter collection. The disintegration most likely occurs during the powerful pressure “blow” when the collected particles are escaping the filter.

The produced particles with **TiO₂ + silica reagent** (20 g/dm³, 3 ml/min; lower concentration than on 1.7.2013 at 12:05; Fig. 4) **with continuous production** on 2.7. at 9:03 were mainly spheres generally larger than 1 μm in diameter. The large spheres consisted of nearly spherical primary particles of approximately up to 50 nm in size (Fig. 4) as in the case of higher reagent concentration (Fig. 4). Thus the size of the spheres ($d_p \approx 1 \mu\text{m}$) did not change but the size of the primary particles seemed to decrease slightly.

Decreasing the reagent concentration further in half with **TiO₂ + silica reagent** (10 g/dm³, 3 ml/min) did not have any significant effect on the size of the agglomerated spheres. The size of the spheres was still generally over 1 μm (Fig. 5).

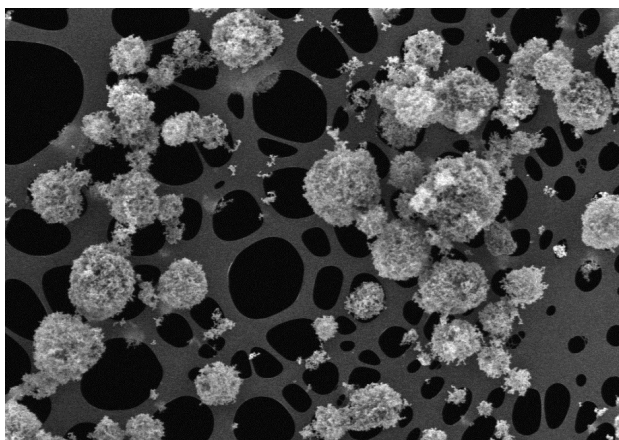


Figure 5a. The generated particles with TiO₂ + silica (20 g/dm³, 3 ml/min) reagent with continuous production (2.7.2013, 9:03). Particles are spheres generally larger than 1 μm in diameter as in Fig. 4.

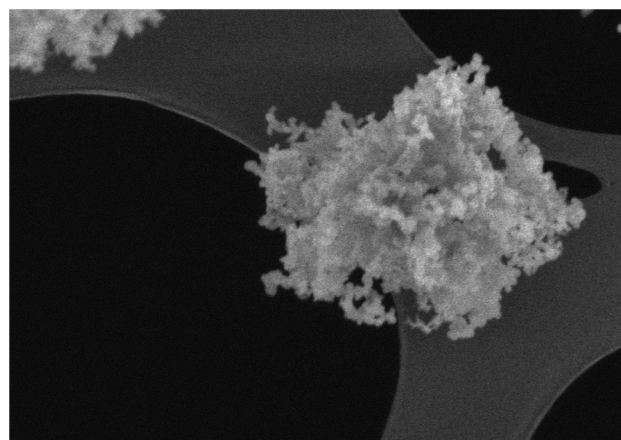


Figure 5b. A detailed image of the sphere. They consist of spherical primary particles of approximately up to 50 nm in diameter. They seem to be slightly smaller than in Fig. 4 (lower concentration).

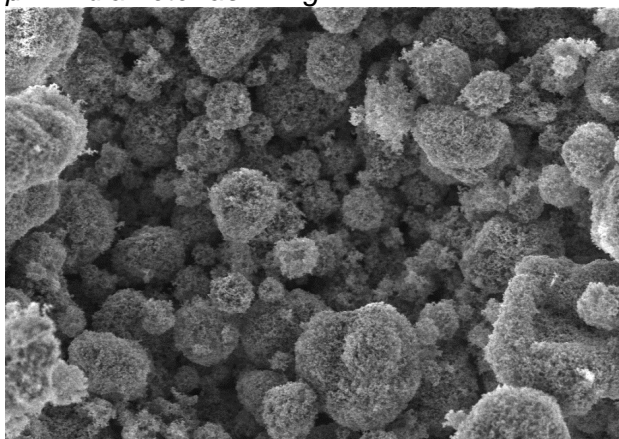


Figure 6a. The generated particles with TiO₂ + silica (10 g/dm³, 3 ml/min) reagent with continuous production (2.7.2013, 9:15). Particles are spheres generally larger than 1 μm in diameter as in Fig. 5.

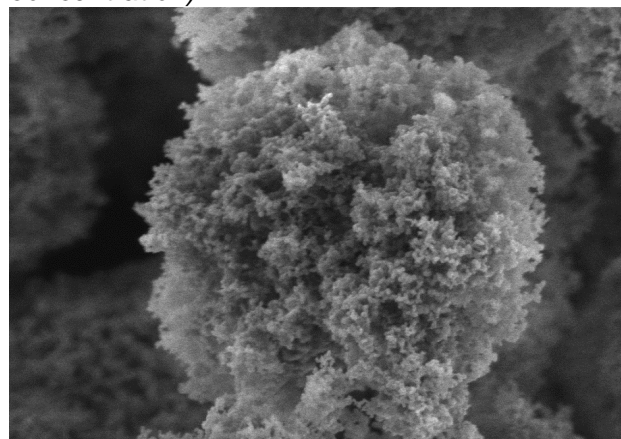


Figure 6b. A detailed image of the sphere. They consist of spherical primary particles of approximately up to 50 nm in diameter, similar size as in Fig. 5.

With **Fe(NO₃)₃·9H₂O + silica** reagent (40 g/dm³, 6 ml/min) with **continuous production** on 1.7. at 12:42 the particles were mainly spheres generally larger than 1 μm in diameter as in the case of TiO₂. The spheres consisted of spherical primary particles of approximately 50 nm in diameter. Larger spheres without any silica on their smooth surface up to approximately 300-500 nm were also seen (Fig. 7). This was discovered in earlier studies with different reagents (Lyyränen, et al., 2011 and 2012).

Decreasing the **Fe (NO₃)₃·9H₂O** reagent (2 g/dm³, 6 ml/min) concentration in to 1/20 did not seem to have any significant effect on the size of the agglomerated spheres as in the case for TiO₂ (Fig. 8). In this case, though, no silica was added. The produced particles, however, looked similar to those produced with silica addition. It is possible that some remains of silica was still left in the particle production lines, even though the lines were cleaned, and cleaning solution was fed through these lines as in all cases when changing the reagent solution. The most probable cause for silica addition type particles is the filter itself: even though the filter

was cleaned before and after each experiment the porosity of the filter stores particles from previous experiment that are nearly impossible to remove completely. This could have been solved by using a new filter material in each experiment. In this case this was not possible because there simply was not enough clean filter material.

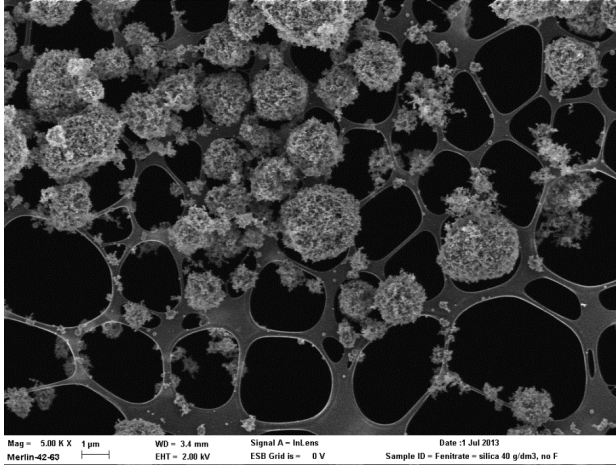


Figure 7a. The generated particles with $\text{Fe}(\text{NO}_3)_3 \cdot 9\text{H}_2\text{O}$ + silica reagent (40 g/dm^3 , 6 ml/min) with continuous production (1.7.2013, 12:42). The particles are nearly spheres generally larger than $1 \mu\text{m}$.

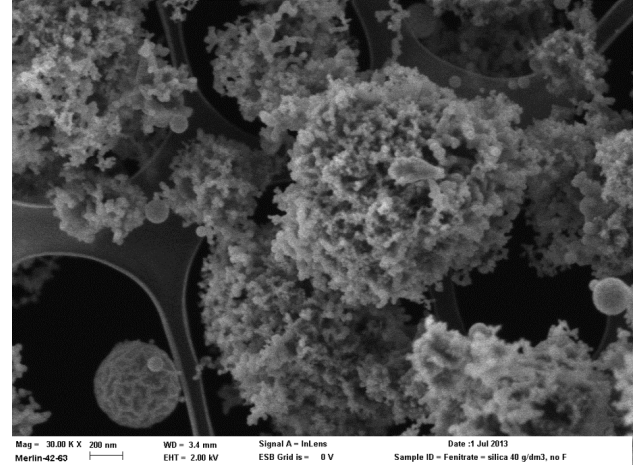


Figure 7b. A detailed image of the spheres. They consist of spherical primary particles of approximately 50 nm in diameter. Larger spheres up to approximately $300\text{-}500 \text{ nm}$ are also seen.

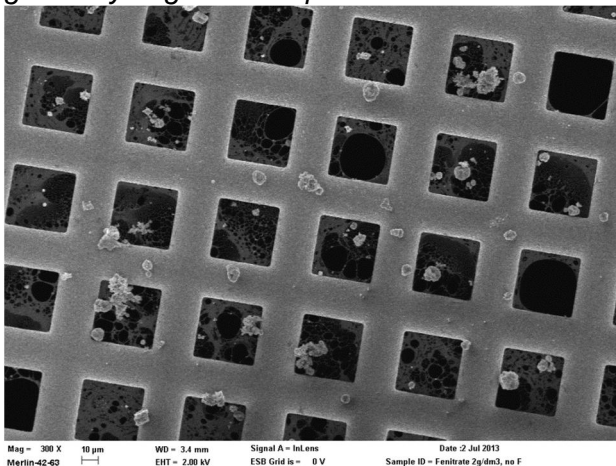


Fig. 8a. The generated particles with $\text{Fe}(\text{NO}_3)_3 \cdot 9\text{H}_2\text{O}$ reagent (2 g/dm^3 , 6 ml/min) with continuous production (2.7.2013, 9:27). Particles are spheres generally larger than $1 \mu\text{m}$ in diameter.

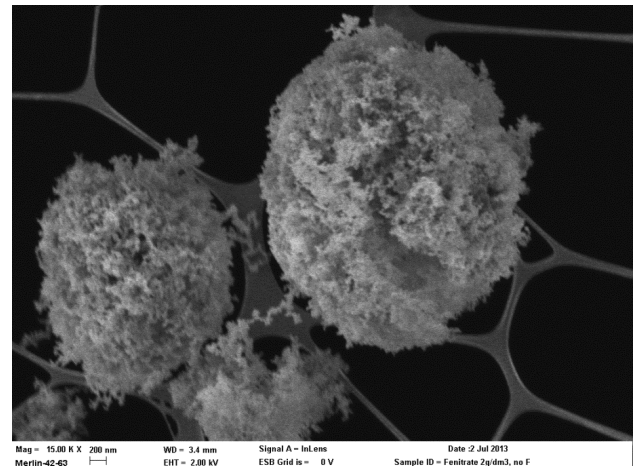


Fig. 8b. A detailed image of the spheres. They consist of spherical primary particles of approximately up to 50 nm in diameter.

With the reference reagent BaCl_2 (5.5 g/dm^3 , 6 ml/min) with **continuous production** the particles were nearly spheres generally larger than $1 \mu\text{m}$ as in previous cases. However, also smaller, approximately from $0.1 \mu\text{m}$ to $0.5 \mu\text{m}$ almost spherical particles were discovered. The structure of the spheres looked highly sintered without any significant microstructure (Fig. 9). The structure is similar as found in the earlier studies (Lyyranen, et al., 2011 and 2012).

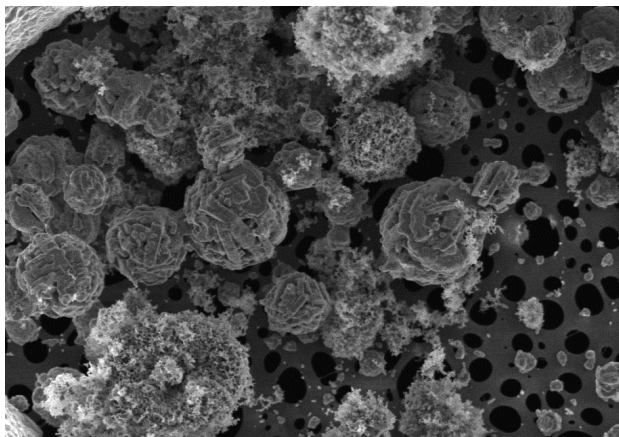


Figure 9a. The generated particles with BaCl_2 (5.5 g/dm^3 , 6 ml/min) with continuous production (1.7.2013, 12:53). Particles are nearly spheres generally larger than $1 \mu\text{m}$.

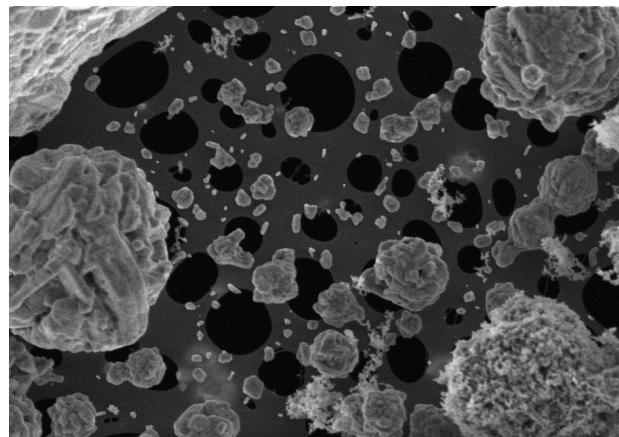


Figure 9b. A detailed image of the spheres. The spheres look sintered. Also smaller spheres are seen.

3.2 Filter collection of particles with heater for TiO_2 , $\text{Fe}(\text{NO}_3)_2 \cdot 9\text{H}_2\text{O}$, BaCl_2 and $\text{Ni}(\text{NO}_3)_2$ with and without silica

3.2.1 Particle number concentration and number size distribution

Typical particle number concentration during the **filter collection with heater for TiO_2 + silica reagent** (20 g/dm^3 , 6 ml/min) on 2.7. at 11:00-11:13 was surprisingly steady, $1.9 \cdot 10^7 \text{ 1/cm}^3$, and the aerodynamic count median diameter (CMD_{ae}) of the particles varied from 0.5 to $0.7 \mu\text{m}$ (Fig. 10a). A SEM sample was also collected. Comparison to the previous corresponding cases without the heater the number concentration was up to 10 times higher, and the produced particles seemed to be smaller in diameter, approximately $0.6 \mu\text{m}$ vs. a few micrometres without the heater.

Decreasing the concentration of **TiO_2 + silica reagent** (20 g/dm^3 , 3 ml/min) on at 11:23-11:30 did not seem to have any significant effect on the particle number concentration or the CMD_{ae} (Fig. 10a).

For **$\text{Fe}(\text{NO}_3)_3 \cdot 9\text{H}_2\text{O}$** (2 g/dm^3 , 6 ml/min) with **filter collection with heater** on 2.7. at 11:43-12:00 the particle number concentration varied between 1.0 - $1.4 \cdot 10^7 \text{ 1/cm}^3$, and the aerodynamic count median diameter (CMD_{ae}) varied from $0.1 \mu\text{m}$ to $0.3 \mu\text{m}$ (Fig. 10a). The CMD_{ae} in this case was almost equal to case without the heater but the activity of the collected particles on the filter was again low. Therefore, no SEM sample collection was considered necessary in this case

Increasing the concentration of **$\text{Fe}(\text{NO}_3)_3 \cdot 9\text{H}_2\text{O}$** (40 g/dm^3 , 6 ml/min) to 40 g/dm^3 on 3.7. at 9:20-9:30 did not increase the value of the highest number concentration but it was more steady at $1.5 \cdot 10^7 \text{ 1/cm}^3$. The CMD_{ae} varied from $0.4 \mu\text{m}$ to $1.0 \mu\text{m}$. This there was a clear increase in the CMD_{ae} probably because of agglomeration (Fig. 10b).

For **BaCl_2** (5.5 g/dm^3 , 6 ml/min) with **filter collection with heater** on 3.7. at 9:41-9:50 the particle number concentration varied between 0.8 - $1.4 \cdot 10^7 \text{ 1/cm}^3$, and the aerodynamic count median diameter (CMD_{ae}) varied from $0.2 \mu\text{m}$ to $3 \mu\text{m}$. The largest particle size (CMD_{ae}) appeared with the first pulse, and the CMD_{ae} of the particles of the following pulses was clearly smaller, on the order of a few hundred nanometres (Fig. 10b).

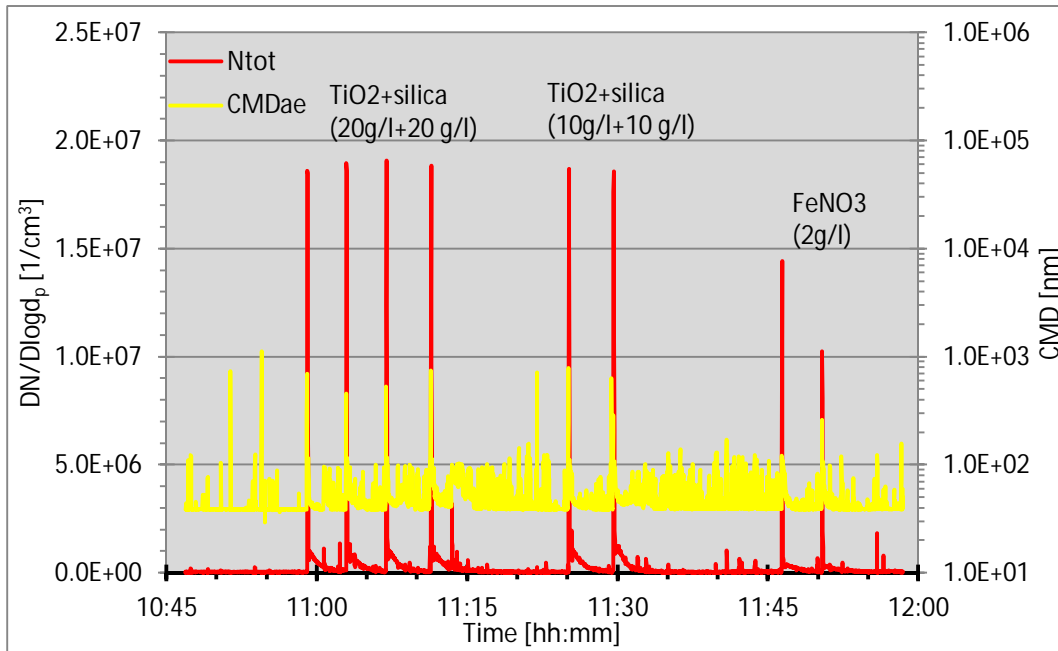


Figure 10a. Total particle number concentration and aerodynamic count median diameter (CMD_{ae}) of the particles generated from TiO_2 + silica and $Fe(NO_3)_3 \cdot 9H_2O$ reagent measured with ELPI on 2.7. 2013, filter collection with heater.

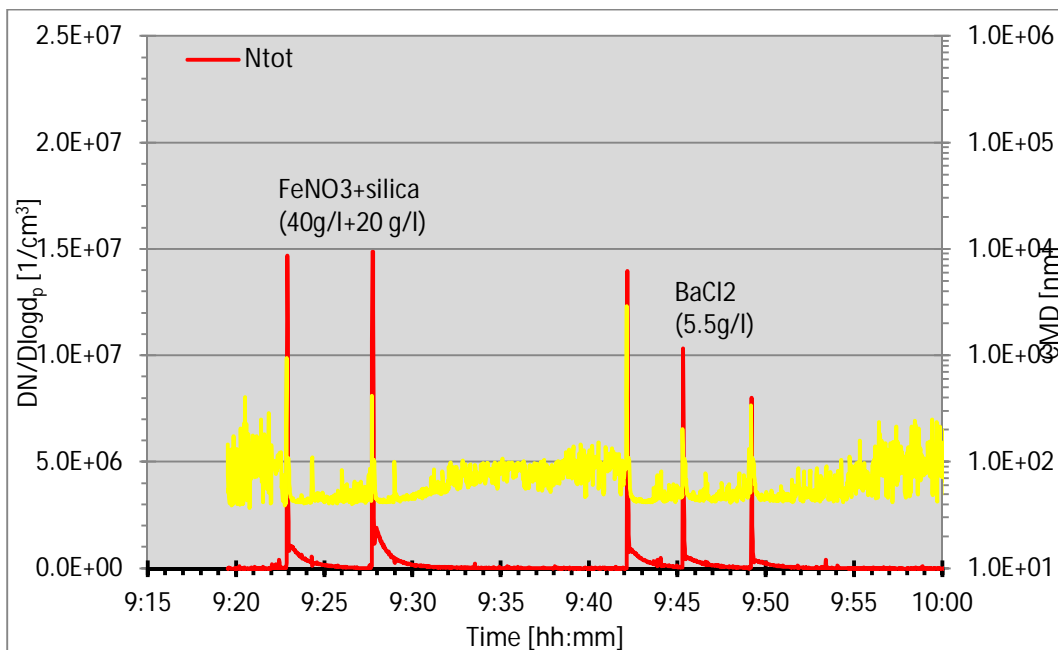


Figure 10b. Total particle number concentration and aerodynamic count median diameter (CMD_{ae}) of the particles generated from $Fe(NO_3)_3 \cdot 9H_2O$ + silica and $BaCl_2$ reagent measured with ELPI on 3.7. 2013, filter collection with heater.

For $Ni(NO_3)_2$ (2 g/dm^3 , 6 ml/min) with **filter collection with heater** on 4.7. at 11:00-11:10 the particle number concentration varied from $4.2 \cdot 10^6 \text{ 1/cm}^3$ to $5.2 \cdot 10^6 \text{ 1/cm}^3$, and the aerodynamic count median diameter (CMD_{ae}) varied from $0.2 \text{ }\mu\text{m}$ to $1 \text{ }\mu\text{m}$ (Fig. 10c). Thus it was almost at the optimal range.

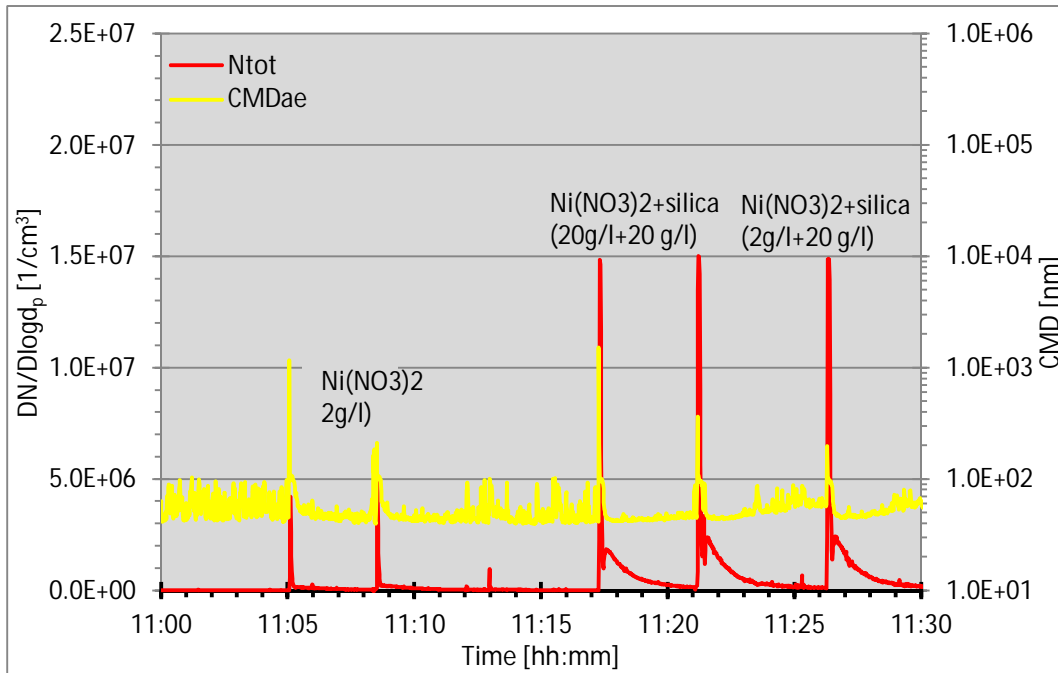


Figure 10c. Total particle number concentration and aerodynamic count median diameter (CMD_{ae}) of the particles generated from $Ni(NO_3)_2$ + silica reagent measured with ELPI on 4.7. 2013, filter collection with heater.

Increasing the concentration of $Ni(NO_3)_2$ (20 g/dm^3 , 6 ml/min) to 20 g/dm^3 on 4.7. at 11:15-11:22 increased the number concentration to $1.5 \cdot 10^7 \text{ 1/cm}^3$, approximately 3-three-fold. This was of the order of magnitude as for TiO_2 ($1.9 \cdot 10^7 \text{ 1/cm}^3$; Fig. 10a). The CMD_{ae} varied from $0.4 \text{ }\mu\text{m}$ to $1.5 \text{ }\mu\text{m}$. Thus there was only a small increase in the CMD_{ae} probably because of some agglomeration (Fig. 10c).

3.2.2 Particle morphology

The produced particles with **TiO_2 + silica reagent** (20 g/dm^3 , 6 ml/min) **with filter collection and heater** on 2.7. at 11:07 were mainly chain-like aggregates as in the case without heater (Fig 11a). The length of the aggregates varied a lot from a few hundred nanometres up to micrometres. This is in congruent with the CMD_{ae} measured with ELPI. The aggregates consisted of nearly spherical primary particles of approximately 50 nm in size (Fig. 11b).

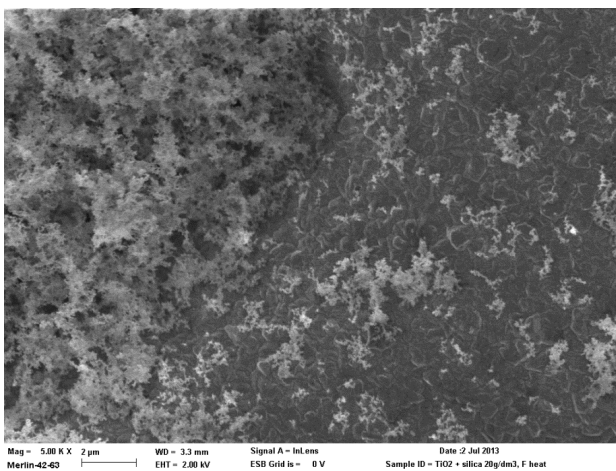


Figure 11a. The generated particles with TiO_2 + silica reagent (20 g/dm^3 , 6 ml/min) with filter and heater (2.7.2013, 11:07). The particles are chain-like aggregates similar to case without

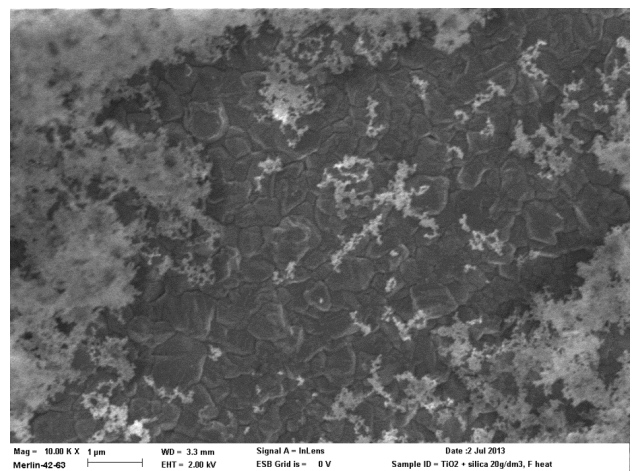


Figure 11b. The aggregates consist of spherical primary particles of approximately 50 nm in diameter as in the case without heater (Fig. 3).

heater (Fig. 3).

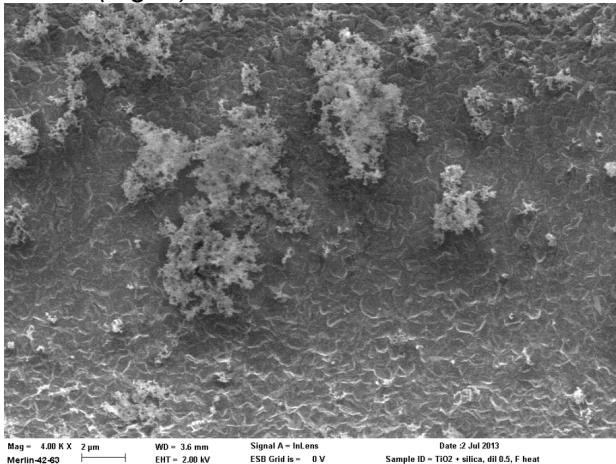


Figure 12a. The generated particles with TiO_2 + silica reagent (20 g/dm^3 , 3 ml/min) with filter and heater (2.7.2013, 11:30). The particles are chain-like aggregates similar to case without heater (Fig. 3).

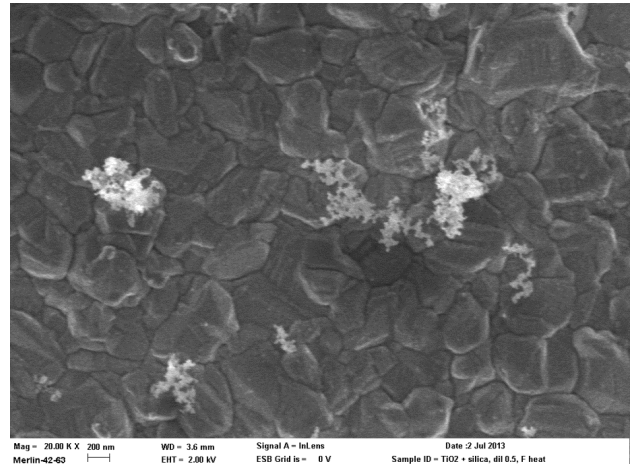


Figure 12b. The aggregates (at smallest approximately $300\text{-}400 \text{ nm}$) consist of spherical primary particles of approximately 50 nm in diameter as in the case without heater (Fig. 3).

Dilution of TiO_2 + silica reagent (20 g/dm^3 , 3 ml/min) in to half with filter collection and heater on 2.7.at 2013, 11:30 did not have any significant effect on the chain-like aggregate or primary particle size (Fig. 12).

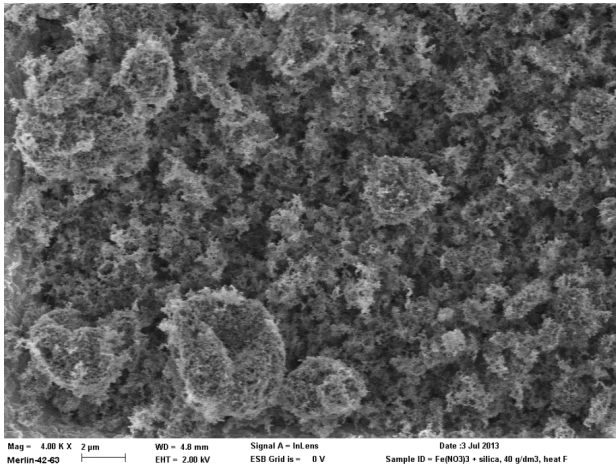


Figure 13a. The generated particles $\text{Fe}(\text{NO}_3)_3 \cdot 9\text{H}_2\text{O}$ + silica reagent (40 g/dm^3 , 6 ml/min) with filter and heater (3.7.2013, 9:28). Particles are nearly spheres generally larger than $1 \mu\text{m}$ as in the case without heater (Fig. 7).

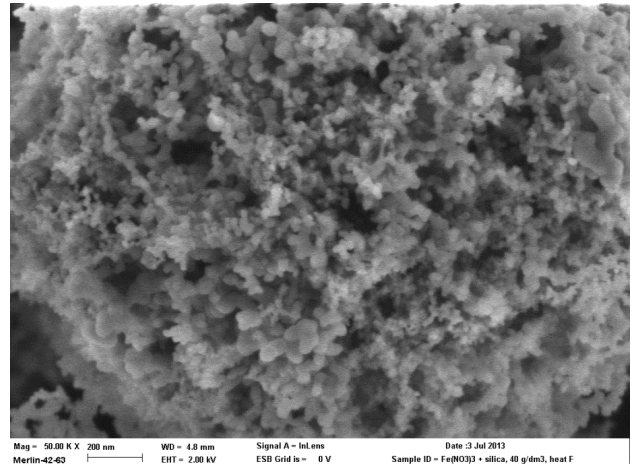


Figure 13b. A detailed image of the spheres. They consist of spherical primary particles of approximately 50 nm in diameter similar to the case without the heater (Fig. 7).

With $\text{Fe}(\text{NO}_3)_3 \cdot 9\text{H}_2\text{O}$ + silica reagent (40 g/dm^3 , 6 ml/min) with filter collection and heater on 3.7. at 9:28 the particles were mainly spheres generally larger than $1 \mu\text{m}$ in diameter as in the case without the heater for both $\text{Fe}(\text{NO}_3)_3 \cdot 9\text{H}_2\text{O}$ and TiO_2 . The spheres consisted of spherical primary particles of approximately 50 nm in diameter (Fig. 13).

SEM sample for the 1/20 diluted $\text{Fe}(\text{NO}_3)_3 \cdot 9\text{H}_2\text{O}$ reagent (2 g/dm^3 , 6 ml/min) was not sampled because the activity of the collected particles was too low. Thus the produced activity signal would have been difficult to filter out from the background noise.

With the reference reagent BaCl_2 (5.5 g/dm^3 , 6 ml/min) with filter collection with heater the particles were mostly chain-like aggregates up to approximately $1 \mu\text{m}$ size (Fig.14a). The

aggregates consisted of small spherical primary particles similar to cases with TiO_2 added silica (e.g., Fig.3 and 11). Thus it is possible that the sample was contaminated with silica. However, the sampling line was always cleaned with several powerful pressure “blows” after each experiment. In addition, TiO_2 reagent was not used directly before or after BaCl_2 . Some spherical particles generally larger than $1\ \mu\text{m}$ in diameter were also seen. The most probable cause for silica contamination was the filter itself: even though the filter was cleaned before and after each experiment the porosity of the filter stores particles from previous experiment that are nearly impossible to remove completely.

For $\text{Ni}(\text{NO}_3)_2$ reagent ($2\ \text{g}/\text{dm}^3$, $6\ \text{ml}/\text{min}$) with **filter collection and heater** on 4.7. at 11:09 the particles were mainly chain-like aggregates similar to TiO_2 + silica (Fig. 11 and 12). The aggregates consisted of spherical primary particles of approximately $50\ \text{nm}$ in diameter (Fig. 15).

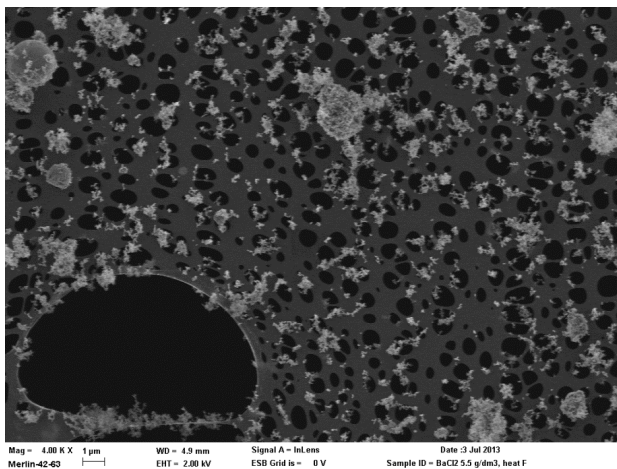


Figure 14a. The generated particles with BaCl_2 ($5.5\ \text{g}/\text{dm}^3$, $6\ \text{ml}/\text{min}$) with filter and heater (3.7.2013, 9:49). Particles are mainly chain-like aggregates up to $1\ \mu\text{m}$ in size. They are not sintered as in the case without heater (Fig. 9)

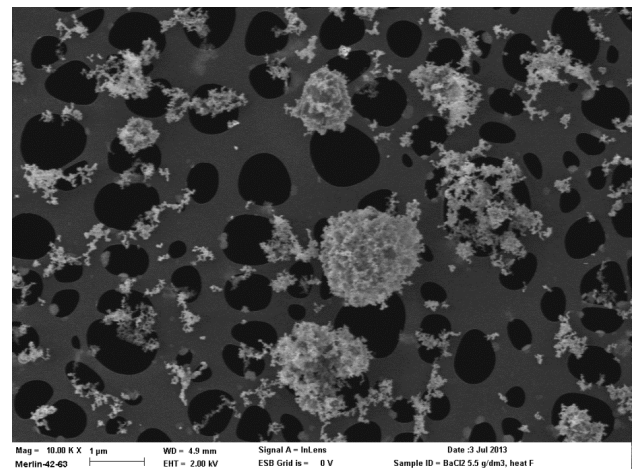


Figure 14b. The size of the aggregates is generally smaller than approximately $1\ \mu\text{m}$. Spherical particles larger than $1\ \mu\text{m}$ are also discovered.

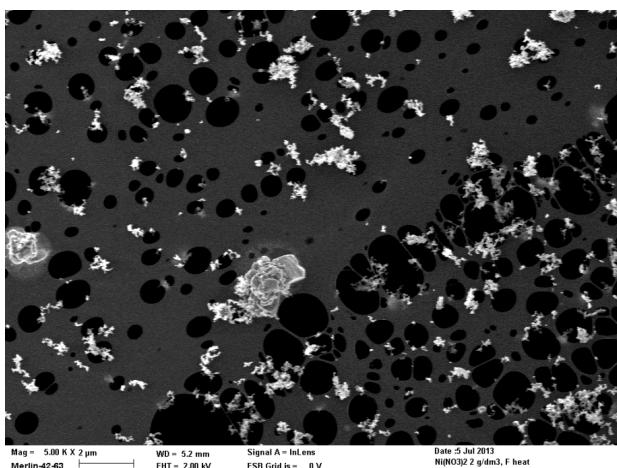


Figure 15a. The generated particles with $\text{Ni}(\text{NO}_3)_2$ reagent ($2\ \text{g}/\text{dm}^3$, $6\ \text{ml}/\text{min}$) with filter and heater (4.7.2013, 11:09). The particles are generally chain-like aggregates similar to TiO_2 + silica (Fig. 11 and 12).

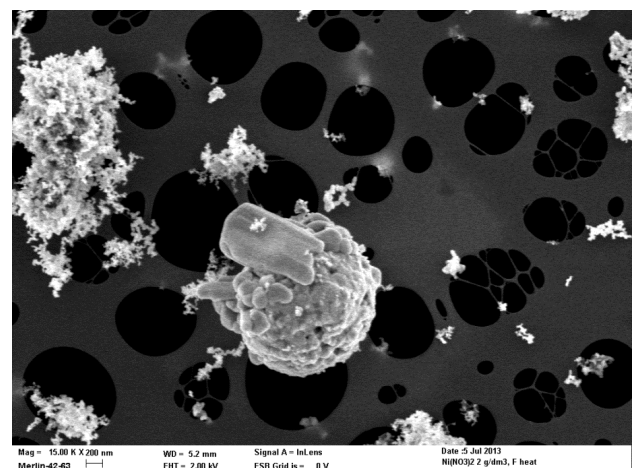


Figure 15b. The aggregates consist of spherical primary particles of approximately $50\ \text{nm}$ in diameter as in the case TiO_2 + silica (Fig. 11 and 12).

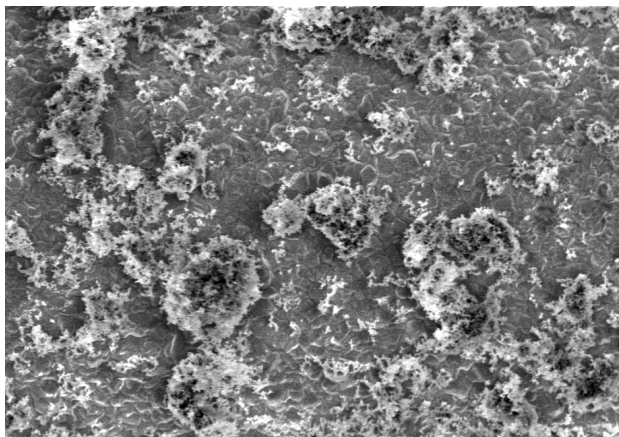


Figure 16a. The generated particles with $\text{Ni}(\text{NO}_3)_2$ + silica reagent (20 g/dm^3 , 6 ml/min) with filter and heater (4.7.2013, 11:21). The particles are chain-like aggregates similar to lower concentration case (Fig. 15), though some spheres larger than $1 \mu\text{m}$ are also seen.

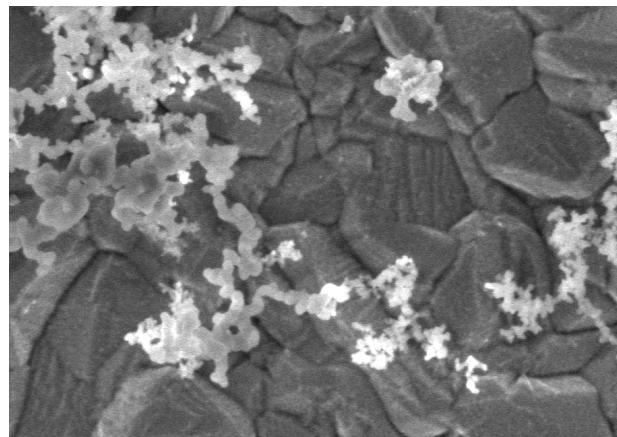


Figure 16b. The aggregates consist of spherical primary particles of approximately 50 nm in diameter similar to lower concentration case (Fig. 15).

Increasing the concentration of $\text{Ni}(\text{NO}_3)_2$ reagent (20 g/dm^3 , 6 ml/min) to 10-fold and adding **silica** with **filter collection and heater** on 4.7. at 11:21 the morphology of the aggregates and the size of the primary particles did not change significantly (Fig. 16). Some spheres larger than $1 \mu\text{m}$ consisting of the primary particles were, though, seen. The structure resembled of that found with $\text{Fe}(\text{NO}_3)_3 \cdot 9\text{H}_2\text{O}$ (Fig. 13).

3.3 Filter collection of particles with heater and with wet inlet tube for TiO_2 , $\text{Fe}(\text{NO}_3)_2 \cdot 9\text{H}_2\text{O}$ and BaCl_2 with and without silica

3.3.1 Particle number concentration and number size distribution

Adding a **wet inlet tube** to simulate possible particle adhesion and retention in systems containing moisture near or at the inlet point for BaCl_2 (5.5 g/dm^3 , 6 ml/min) with **filter collection and heater** caused a clear decrease in total particle number concentration to $3.7\text{--}5.4 \cdot 10^6 \text{ 1/cm}^3$, approximately 2.5-fold decrease compared to the case without the wet tube. This was a clear indication of particles being trapped by the wet inlet tube. The CMD_{ae} seemed to slightly increase between $0.7\text{--}4 \mu\text{m}$ (Fig. 17).

For $\text{Fe}(\text{NO}_3)_3 \cdot 9\text{H}_2\text{O}$ + silica (40 g/dm^3 , 6 ml/min) with **filter collection with heater** and with a **wet inlet tube** the number concentration of the pulse on 3.7. at 10:32 was low, $3.4 \cdot 10^6 \text{ 1/cm}^3$, but the second at 10:35 was almost equal to case without the wet inlet tube, $1.5 \cdot 10^7 \text{ 1/cm}^3$ (Fig. 17). It seemed that during the first pulse the filter was not saturated, and the particles were not able to escape the filter. Another explanation for this would be the saturation of the wet inlet tube by the particles. This, however, is not probable because the tube was wetted after each experiment. It also possible that the wetting of the tube was insufficient thus allowing the penetration of large particles (on the order a few micrometres). The CMD_{ae} varied between $1\text{--}3 \mu\text{m}$ (Fig. 17). Thus the particles were clearly larger ($0.4\text{--}1 \mu\text{m}$ vs. $1\text{--}3 \mu\text{m}$) probably because of trapping some moisture and agglomerating when travelling through the wet inlet tube.

Because of the large variation in the measured particle number concentration of $\text{Fe}(\text{NO}_3)_3 \cdot 9\text{H}_2\text{O}$ + silica (40 g/dm^3 , 6 ml/min) with **filter collection with heater** and with a **wet inlet tube** it was measured again at 11:10–11:15. The number concentration was $1.4 \cdot 10^7 \text{ 1/cm}^3$, and the CMD_{ae} was $0.2 \mu\text{m}$ (Fig. 17). The number concentration was thus almost

equal to the previous measurement at 10:35, but the CMD_{ae} was clearly smaller, $1.4 \mu\text{m}$ vs. $0.2 \mu\text{m}$. This would indicate that the surface of the tube was not sufficiently wetted thus allowing the penetration of the large particles.

Decreasing the $\text{Fe}(\text{NO}_3)_3 \cdot 9\text{H}_2\text{O}$ (2 g/dm^3 , 6 ml/min) reagent concentration at 11:45-11:55 from 40 g/dm^3 to 2 g/dm^3 caused the number concentration to decrease to $1.0 \cdot 10^7 \text{ 1/cm}^3$ from $1.0\text{-}1.4 \cdot 10^7 \text{ 1/cm}^3$, thus on average less than 20 %. The CMD_{ae} was $0.2 \mu\text{m}$, and was thus equal to the case with higher reagent concentration (Fig.17).

For $\text{TiO}_2 + \text{silica}$ (20 g/dm^3 , 6 ml/min) with **filter collection with heater** and with a **wet inlet tube** the number concentration on 3.7 at 10:53-11:03 varied between $1.4\text{-}1.5 \cdot 10^7 \text{ 1/cm}^3$, and CMD_{ae} varied between $0.2\text{-}0.6 \mu\text{m}$ (Fig. 17). Comparison to the case without the wet inlet tube (Fig. 3) the number concentration decreased slightly, from $1.9 \cdot 10^7 \text{ 1/cm}^3$ to $1.5 \cdot 10^7 \text{ 1/cm}^3$. Thus some trapping of the particles by the wet inlet tube was probable.

Decreasing the $\text{TiO}_2 + \text{silica}$ (20 g/dm^3 , 3 ml/min) reagent concentration at 11:30-11:40 caused the number concentration to decrease to $1.1 \cdot 10^7 \text{ 1/cm}^3$, that is the number concentration nearly halved (Fig. 17). The CMD_{ae} was $0.3 \mu\text{m}$ thus basically the same as with the higher concentration case.

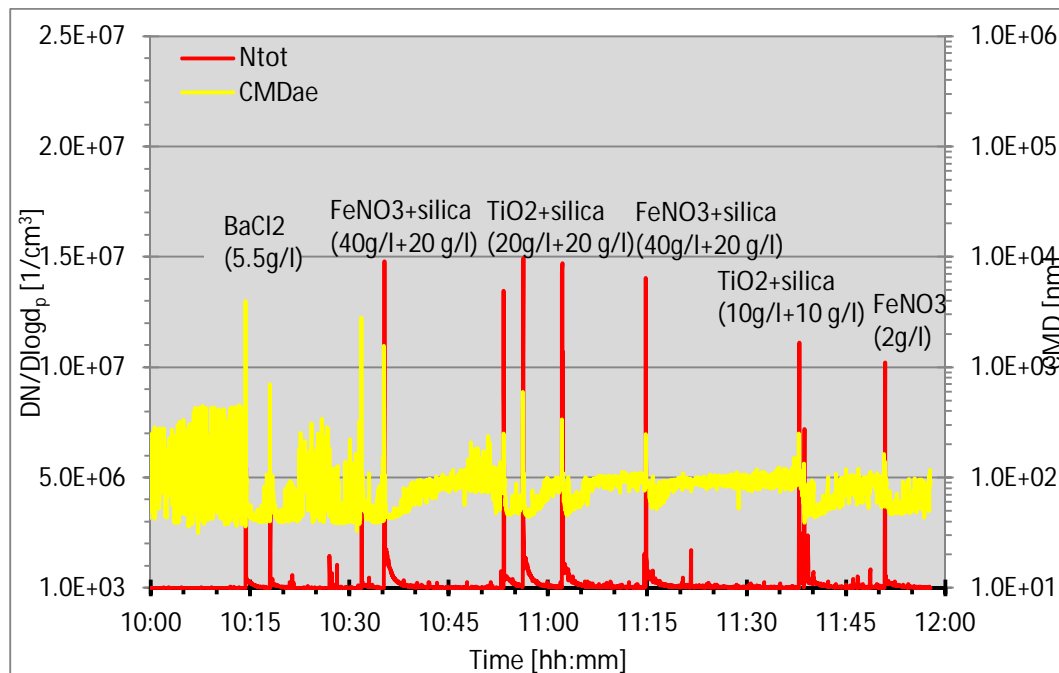


Figure 17. Total particle number concentration and aerodynamic count median diameter (CMD_{ae}) of the particles generated from $\text{Fe}(\text{NO}_3)_3 \cdot 9\text{H}_2\text{O}$, TiO_2 and BaCl_2 with or without silica measured with ELPI on 3.7. 2013, filter collection with heater and with an addition of a wet inlet tube simulating possible particle adhesion and retention in systems containing moisture near or at the inlet point.

3.3.2 Particle morphology

With a **wet inlet tube** to simulate possible particle adhesion and retention in systems containing moisture near or at the inlet point for BaCl_2 (5.5 g/dm^3 , 6 ml/min) with **filter collection with heater** on 3.7. at 10:18 similar structures as without the wet inlet tube were discovered (Fig. 18). However, the portion of the almost spherical aggregates generally larger than $1 \mu\text{m}$ seemed to be higher than without the wet tube (Fig. 14).

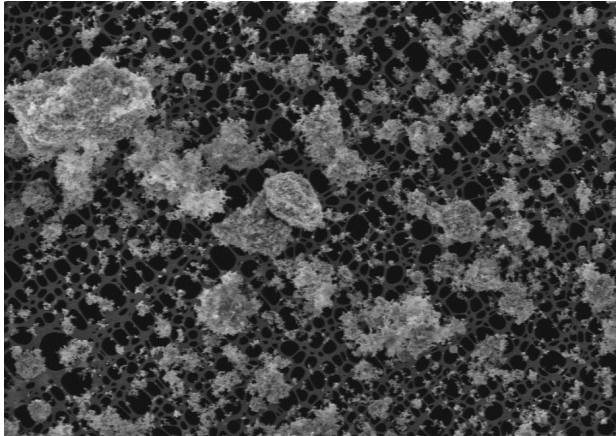


Figure 18a. The generated particles with BaCl_2 (5.5 g/dm^3 , 6 ml/min) with filter, heater and wet inlet tube (3.7.2013, 10:18). Particles mainly chain-like aggregates up to $1 \mu\text{m}$ in size or almost spheres larger than $1 \mu\text{m}$. They are not sintered as in the case without heater (Fig. 9)

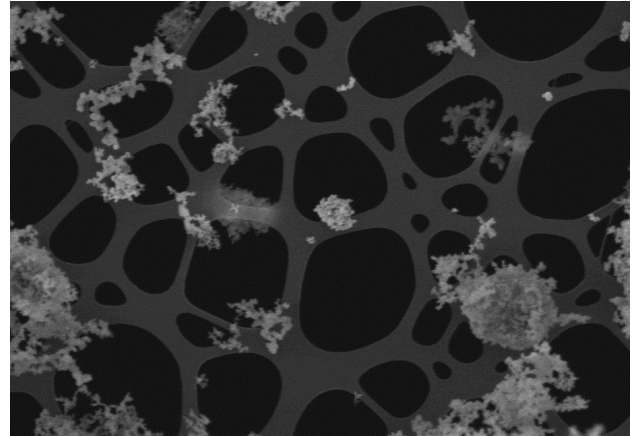


Figure 18b. The size of the aggregates is generally smaller than approximately $1 \mu\text{m}$. They consist of almost spherical particles approximately 50 nm in diameter.

For $\text{Fe}(\text{NO}_3)_3 \cdot 9\text{H}_2\text{O} + \text{silica}$ (40 g/dm^3 , 6 ml/min) with **filter collection, heater** and with a **wet inlet tube** on 3.7. at 10:35 the particles were mainly spheres generally larger than $1 \mu\text{m}$ in diameter as in the case without the wet inlet tube (Fig. 13). The spheres consisted of spherical primary particles of approximately 50 nm in diameter (Fig. 19a and 19b). This indicated that that the wetting of the inlet tube may have been insufficient because basically no trapping of particles had occurred. Therefore, the experiment was repeated at 11:15, and the size of the penetrated particles was found to be smaller (19c and 19d) as in the case of ELPI measurement (Fig. 17 at 11:15 vs. 10:35, yellow curve).

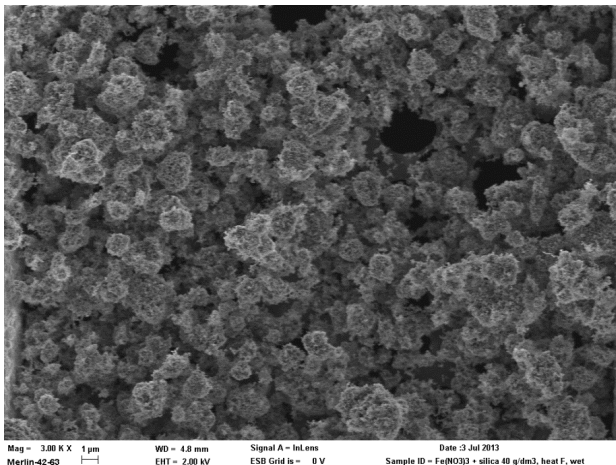


Figure 19a. The generated particles $\text{Fe}(\text{NO}_3)_3 \cdot 9\text{H}_2\text{O} + \text{silica}$ reagent (40 g/dm^3 , 6 ml/min) with filter, heater and wet inlet tube (3.7.2013, 10:35). Particles are nearly spheres generally larger than $1 \mu\text{m}$ as in the case without the wet inlet tube (Fig. 13).

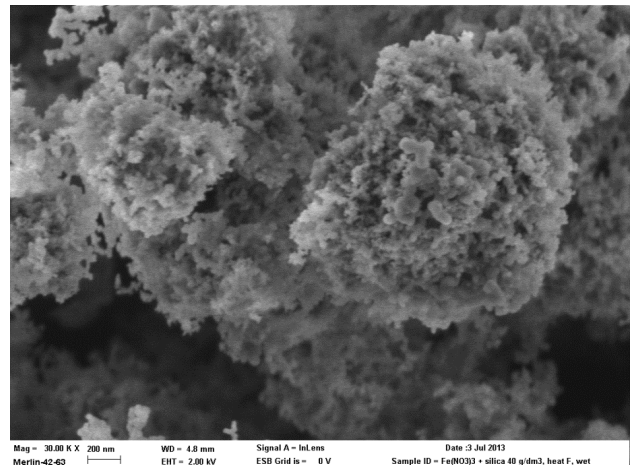


Figure 19b. A detailed image of the spheres. They consist of spherical primary particles of approximately 50 nm in diameter similar to the case without the wet inlet tube (Fig. 13).

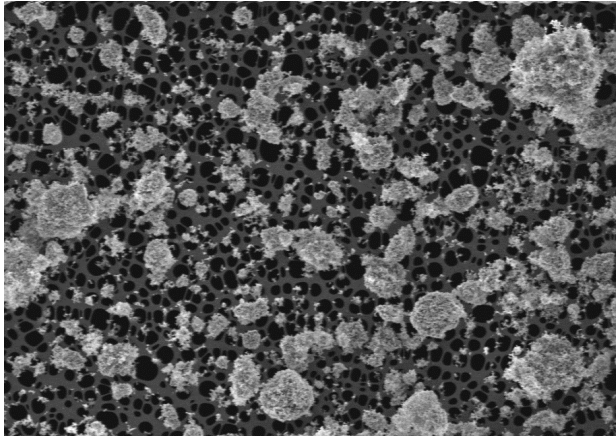


Figure 19c. The generated particles $\text{Fe}(\text{NO}_3)_3 \cdot 9\text{H}_2\text{O}$ + silica reagent (40 g/dm^3 , 6 ml/min) with filter, heater and wet inlet tube (3.7.2013, 11:15). Particles seemed to be smaller than in the earlier $\text{Fe}(\text{NO}_3)_3 \cdot 9\text{H}_2\text{O}$ case (Fig. 19).

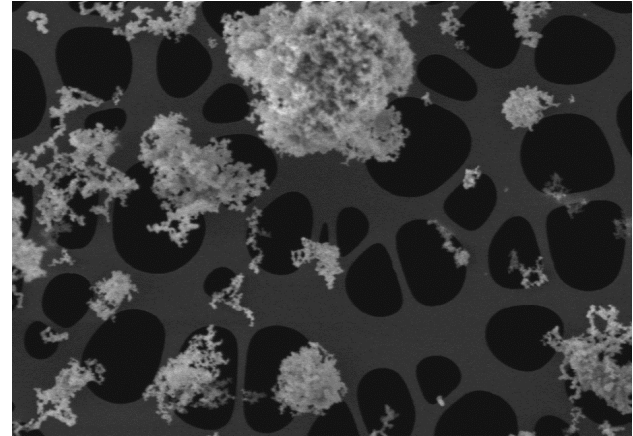


Figure 19d. A detailed image of the aggregates. They consist of spherical primary particles of approximately 50 nm in diameter similar to the earlier $\text{Fe}(\text{NO}_3)_3 \cdot 9\text{H}_2\text{O}$ case (Fig. 19).

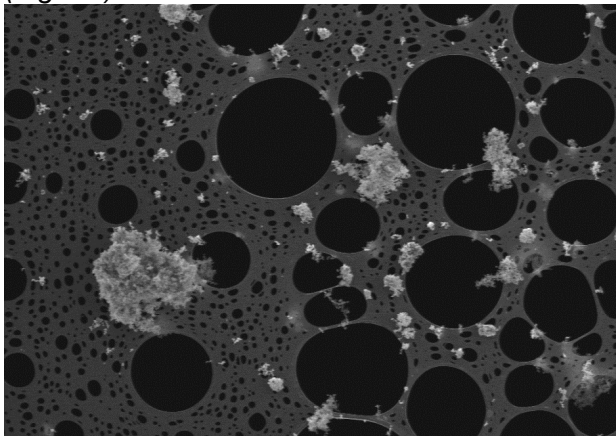


Figure 20a. The generated particles $\text{Fe}(\text{NO}_3)_3 \cdot 9\text{H}_2\text{O}$ reagent (2 g/dm^3 , 6 ml/min) with filter, heater and wet inlet tube (3.7.2013, 11:51). Similar structures as with 40 g/dm^3 but in lower concentration are found (Fig. 19).

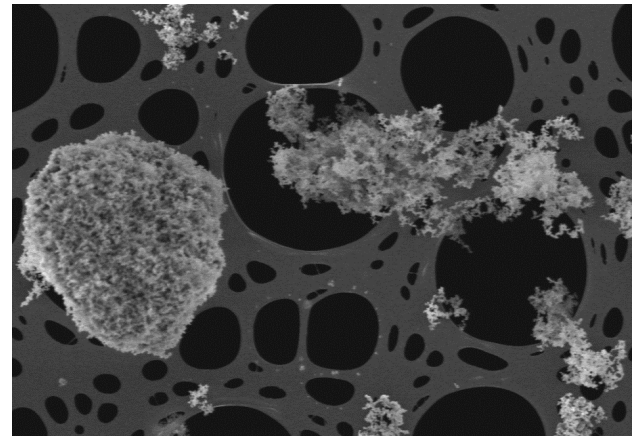


Figure 20b. A detailed image of the aggregates. They consist of spherical primary particles of approximately 50 nm in diameter similar to the earlier $\text{Fe}(\text{NO}_3)_3 \cdot 9\text{H}_2\text{O}$ case (Fig. 19).

Decreasing the $\text{Fe}(\text{NO}_3)_3 \cdot 9\text{H}_2\text{O}$ (2 g/dm^3 , 6 ml/min) reagent concentration at 11:51 from 40 g/dm^3 to 2 g/dm^3 caused a clear decrease in the number of the penetrated particles and their size (Fig.20). Some larger particles ($> 1 \mu\text{m}$) were still able to penetrate the wet inlet tube. The structure of the particles resembled the one with added silica. Thus it would seem that some silica was left in the wet inlet tube regardless of the cleaning of this tube. Another cause was that some silica containing particles reentrained from the surfaces of the measurement line after inlet point (Fig. 1b and 1c). However, the most probable cause for silica contamination was the filter itself: even though the filter was cleaned before and after each experiment the porosity of the filter stores particles from previous experiment that are nearly impossible to remove completely.

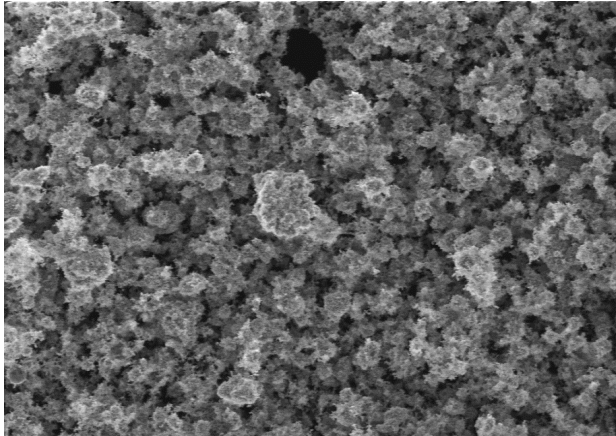


Figure 21a. The generated particles with TiO_2 + silica reagent (20 g/dm^3 , 6 ml/min) with filter, heater and wet inlet tube (3.7.2013, 11:02). The particles are spherical aggregates similar to $\text{Fe}(\text{NO}_3)_3 \cdot 9\text{H}_2\text{O}$ (Fig. 19).

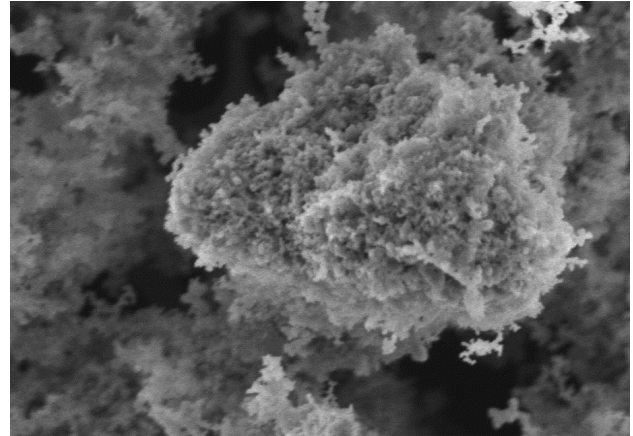


Figure 21b. The aggregates consist of spherical primary particles of approximately 50 nm in diameter.

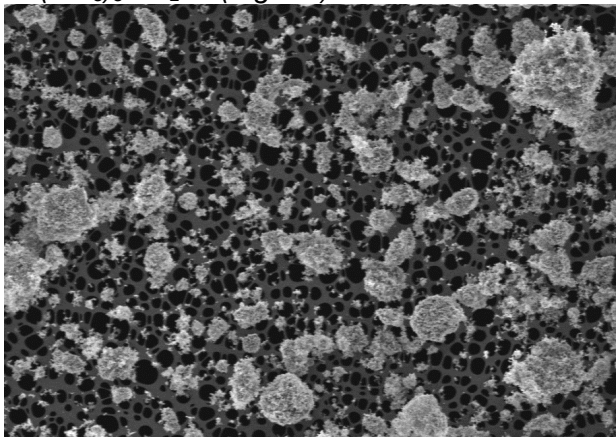


Figure 22a. The generated particles with TiO_2 + silica reagent (20 g/dm^3 , 3 ml/min) with filter, heater and wet inlet tube (3.7.2013, 11:38). The particles are similar to high concentration case (Fig. 21) but maybe slightly smaller.

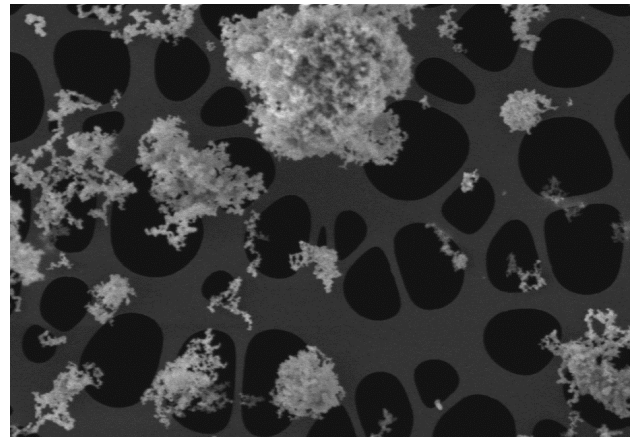


Figure 22b. The aggregates consist of spherical primary particles of approximately 50 nm in diameter as in the high concentration case (Fig. 3).

The produced particles with **TiO_2 + silica reagent** (20 g/dm^3 , 6 ml/min) **with filter collection, heater and wet inlet tube** on 3.7. at 11:02 were mainly spherical aggregates larger than approximately $1 \mu\text{m}$ in diameter as in the case with $\text{Fe}(\text{NO}_3)_3 \cdot 9\text{H}_2\text{O}$ (Fig 19). This is in contradiction with the case without the wet inlet tube, where the particles were mainly chain-like aggregates. It possible that remains of the previous experiment $\text{Fe}(\text{NO}_3)_3 \cdot 9\text{H}_2\text{O}$ particles reentrained from the surfaces of the inlet tube or sampling line (Fig. 1b and 1c). The most probable cause for silica contamination was the filter itself: even though the filter was cleaned before and after each experiment the porosity of the filter stores particles from previous experiment that are nearly impossible to remove completely.

Dilution of **TiO_2 + silica reagent** (20 g/dm^3 , 3 ml/min) in to half **with filter collection and heater** on 3.7.at 2013, 11:38 did not have any significant effect on the size of the aggregates or primary particle size (Fig. 22). However, the number of penetrated particles seemed to be lower, and their size slightly smaller.

3.4 Filter collection of particles with heater and with spirial inlet tube for TiO_2 , $\text{Fe}(\text{NO}_3)_2 \cdot 9\text{H}_2\text{O}$ and BaCl_2 with and without silica

3.4.1 Particle number concentration and number size distribution

Adding a **spiral inlet tube** to simulate particle adhesion and retention caused by a non-optimal inlet tube for **$\text{Fe}(\text{NO}_3)_3 \cdot 9\text{H}_2\text{O}$** (2 g/dm^3 , 6 ml/min) reagent with **filter collection and heater** on 4.7. at 9:40-9:50 caused a severe decrease of up to two orders of magnitude in total particle number concentration down to $1.3 \cdot 10^5 \text{ 1/cm}^3$ (Fig. 23) compared to the case without the spiral inlet tube (Fig. 10a). The count median diameter (CMD_{ae}) of the penetrated particles was $0.4 \text{ }\mu\text{m}$ (Fig. 23) thus of the same order of magnitude as in the case without the spiral inlet tube ($0.1\text{-}0.3 \text{ }\mu\text{m}$; Fig. 10a).

Increasing the **$\text{Fe}(\text{NO}_3)_3 \cdot 9\text{H}_2\text{O}$** (40 g/dm^3 , 6 ml/min) to 20-fold and adding **silica** at 10:30-10:40 caused the number concentration to increase from $1.3 \cdot 10^5 \text{ 1/cm}^3$ to $5.4\text{-}5.9 \cdot 10^6 \text{ 1/cm}^3$ thus being up to almost 50-fold (Fig.23). Compared to the case without the spiral tube the number concentration decreased approximately to 1/3. The (CMD_{ae}) was almost the same as without the spiral tube (Fig. 10a).

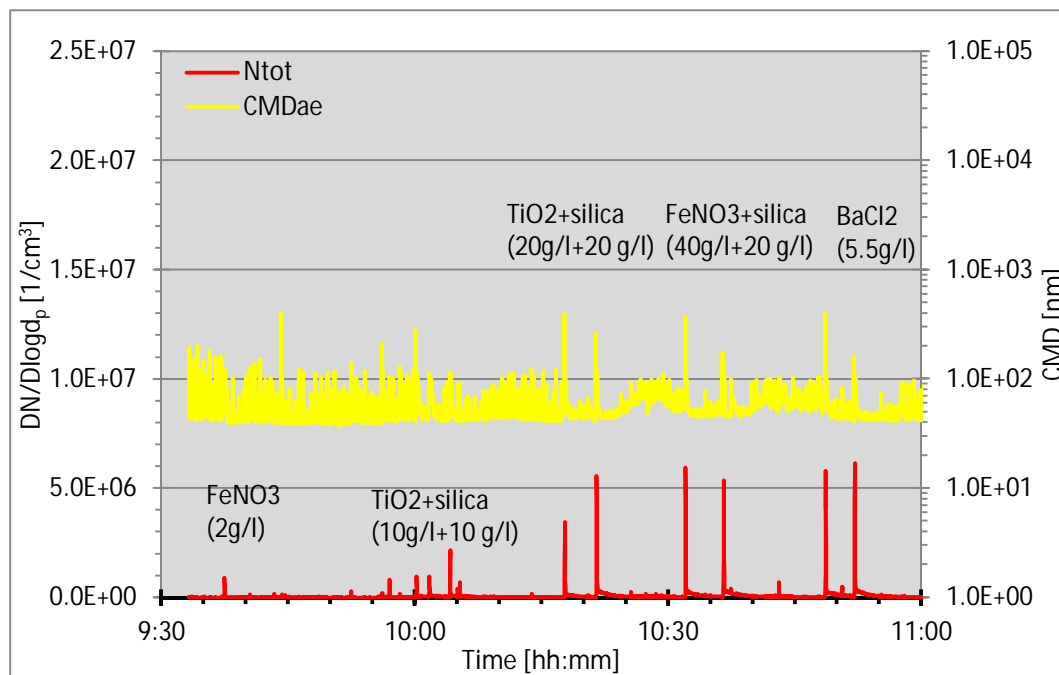


Figure 23. Total particle number concentration and aerodynamic count median diameter (CMD_{ae}) of the particles generated from $\text{Fe}(\text{NO}_3)_3 \cdot 9\text{H}_2\text{O}$, TiO_2 and BaCl_2 with or without silica measured with ELPI on 4.7. 2013, filter collection with heater and with an addition of a spiral inlet tube simulating particle adhesion and retention caused by a non-optimal inlet tube.

For **$\text{TiO}_2 + \text{silica}$** (10 g/dm^3 , 6 ml/min) with **filter collection, heater** and with a **spiral inlet tube** the number concentration on 4.7 at 9:55-10:05 varied from $8.2 \cdot 10^5 \text{ 1/cm}^3$ to $9.5 \cdot 10^5 \text{ 1/cm}^3$ being thus nearly 20-fold lower with spiral inlet tube (Fig. 23). Thus severe trapping of the particles by the spiral inlet tube occurred. The CMD_{ae} varied between $0.2\text{-}0.3 \text{ }\mu\text{m}$ being thus slightly smaller than without the spiral tube ($0.5\text{-}0.7 \text{ }\mu\text{m}$, Fig. 10a)

Increasing the **$\text{TiO}_2 + \text{silica}$** (20 g/dm^3 , 3 ml/min) reagent concentration by a factor of two at 10:15-10:22 increased the number concentration to $3.3\text{-}5.6 \cdot 10^6 \text{ 1/cm}^3$ thus varying between 3.5- and 7-fold compared with lower TiO_2 reagent concentration (Fig. 23). Again, significant trapping of the particles (number concentration without the spiral tube $1.9 \cdot 10^6 \text{ 1/cm}^3$) by the spiral inlet tube occurred. The CMD_{ae} varied between $0.3\text{-}0.4$ being thus slightly larger than with lower concentration.

For BaCl_2 (5.5 g/dm^3 , 6 ml/min) with **filter collection, heater and spiral inlet tube** on 4.7. at 10:45-10:55 the particle number concentration varied from $5.8 \cdot 10^6 \text{ 1/cm}^3$ to $6.1 \cdot 10^6 \text{ 1/cm}^3$ being thus approximately 2-fold lower than without the spiral tube, and of the same order with $\text{TiO}_2 + \text{silica}$ (20 g/dm^3 , 3 ml/min) reagent (Fig. 23). Thus clear trapping of the particles by the spiral inlet tube occurred. The (CMD_{ae}) varied from $0.2\text{-}0.4 \text{ }\mu\text{m}$ being thus almost equal with the case without the spiral tube if the first pulse of this case is ignored (Fig. 10b).

3.4.2 Particle morphology

With a **spiral inlet tube** for $\text{Fe}(\text{NO}_3)_3 \cdot 9\text{H}_2\text{O}$ (2 g/dm^3 , 6 ml/min) with **filter collection and heater** on 4.7. at 9:45 the number of the observed particles was really low thus indicating severe trapping of the spiral inlet tube (Fig. 24). The penetrated particles were of many different shapes.

Increasing the reagent concentration of $\text{Fe}(\text{NO}_3)_3 \cdot 9\text{H}_2\text{O}$ (40 g/dm^3 , 6 ml/min) to 20-fold and adding **silica** increased then number of the penetrated particles. The particles were chain-like and spherical aggregates generally larger than $1 \text{ }\mu\text{m}$ in diameter. The aggregates consisted of small almost spherical primary particles of approximately 50 nm in diameter (Fig. 25).

The produced particles with $\text{TiO}_2 + \text{silica}$ reagent (10 g/dm^3 , 6 ml/min) with **filter collection, heater and spiral inlet tube** on 4.7. at 10:00 were mainly chain-like aggregates generally smaller than μm in size. Moreover, the number of the particles was low thus indicating severe trapping by the spiral inlet tube (Fig. 26).

Doubling the reagent concentration of $\text{TiO}_2 + \text{silica}$ reagent (20 g/dm^3 , 6 ml/min) to 20 mg/dm^3 increased the number of the penetrated particles. In addition, the particles were no longer only chain-like aggregates but also almost spherical particles generally larger than $1 \text{ }\mu\text{m}$ in diameter were observed (Fig. 27). The morphology was surprisingly similar to that with $\text{Fe}(\text{NO}_3)_3 \cdot 9\text{H}_2\text{O}$ and silica (Fig. 25).

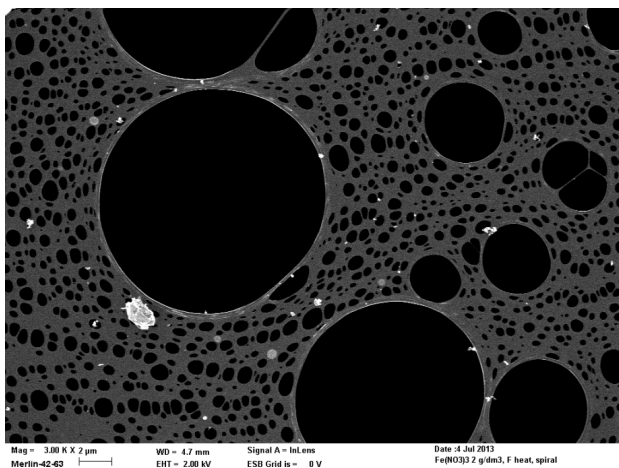


Figure 24a. The generated particles $\text{Fe}(\text{NO}_3)_3 \cdot 9\text{H}_2\text{O}$ reagent (2 g/dm^3 , 6 ml/min) with filter, heater and spiral inlet tube (4.7.2013, 9:45). Only very few particles of different shapes are seen.

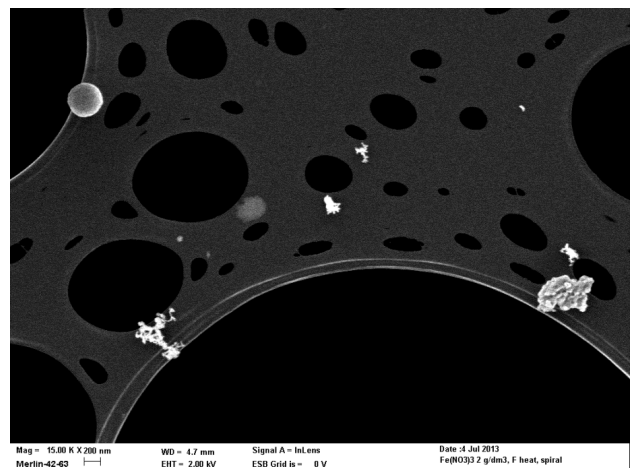


Figure 24b. Any different shapes of particles are observed, and the number of particles is low thus indicating severe trapping by the spiral inlet tube.

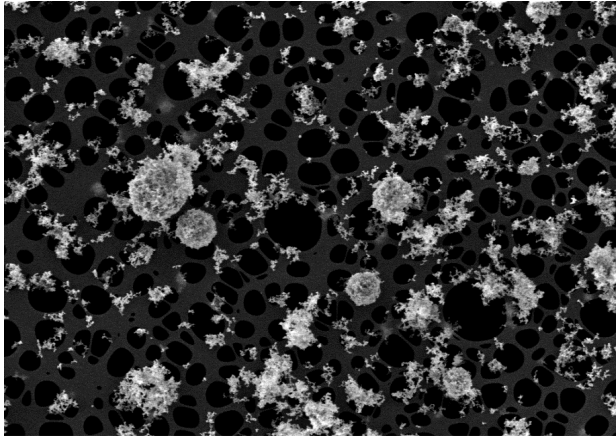


Figure 25c. The generated particles $\text{Fe}(\text{NO}_3)_3 \cdot 9\text{H}_2\text{O}$ + silica reagent (40 g/dm^3 , 6 ml/min) with filter, heater and spiral inlet tube (4.7.2013, 10:37). Particles are spherical ($> 1 \mu\text{m}$) or chain-like aggregates.

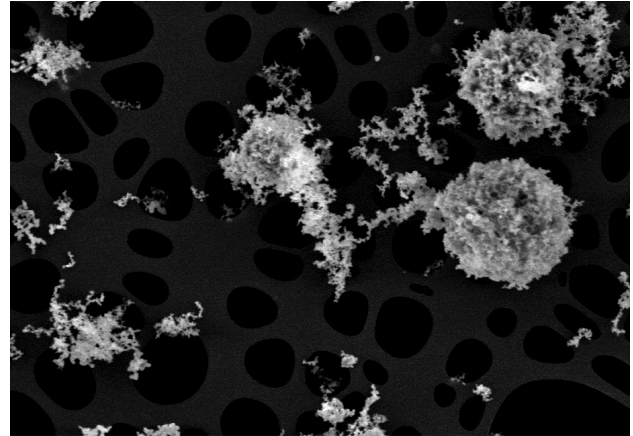


Figure 25d. A detailed image of the aggregates. They consist of spherical primary particles of approximately 50 nm in diameter similar to the earlier $\text{Fe}(\text{NO}_3)_3 \cdot 9\text{H}_2\text{O}$ case (Fig. 19).

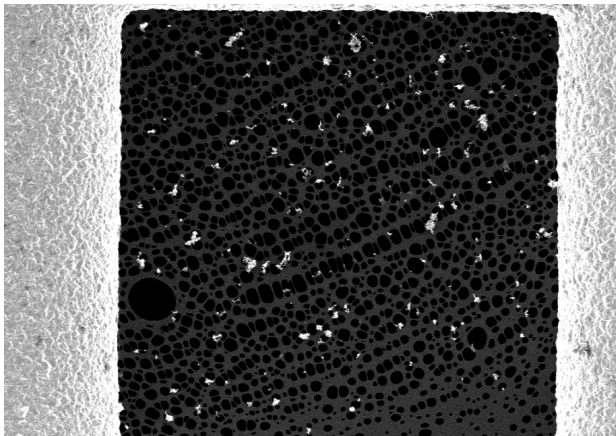


Figure 26a. The generated particles with TiO_2 + silica reagent (10 g/dm^3 , 6 ml/min) with filter, heater and spiral inlet tube (4.7.2013, 10:00). The particles are chain-like aggregates.

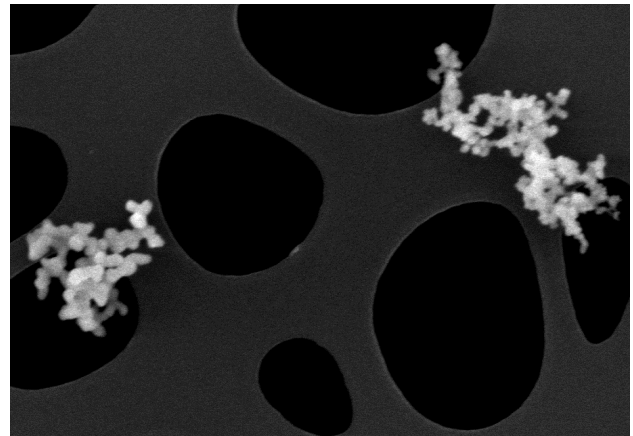


Figure 26b. The aggregates consist of spherical primary particles of approximately 50 nm in diameter.

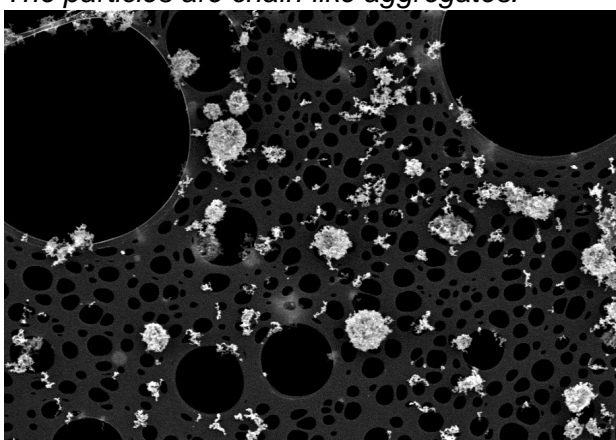


Figure 27a. The generated particles with TiO_2 + silica reagent (20 g/dm^3 , 6 ml/min) with filter, heater and spiral inlet tube (4.7.2013, 10:21). The particles are chain-like and spherical aggregates.

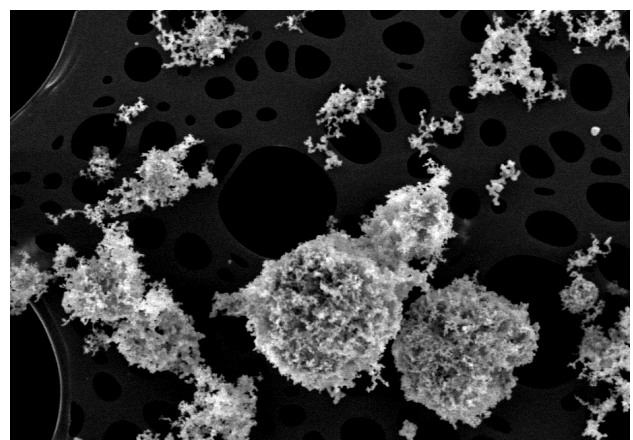


Figure 27b. The aggregates consist of spherical primary particles of approximately 50 nm in diameter.

For BaCl_2 (5.5 g/dm^3 , 6 ml/min) with **filter collection, heater and spiral inlet tube** on 4.7. at 10:52 the particles were chain-like and nearly spherical aggregates generally larger than $1 \mu\text{m}$ (Fig. 28). The number of the particles was clearly lower than without the spiral inlet tube thus indicating once again the efficient particle trapping of the spiral inlet tube.

The morphology of the particles reminded of that for particles with added silica (e.g. Fig. 3 and 11) but not that of pure BaCl_2 (Fig. 9). It is possible that some silica containing particles from previous experiments have reentrained from the spiral tube during the pressure “blow”. However, this is not very probable because the inlet tube was cleaned by several pressure “blows” before and after each experiment. The most probable cause for the silica contamination is the filter itself: even though it was also cleaned by several pressure “blows” before and after each experiment the porosity of the filter material will store particles from previous experiments that may escape during the following experiment(s). The change of the filter material after each experiment would have solved the problem.

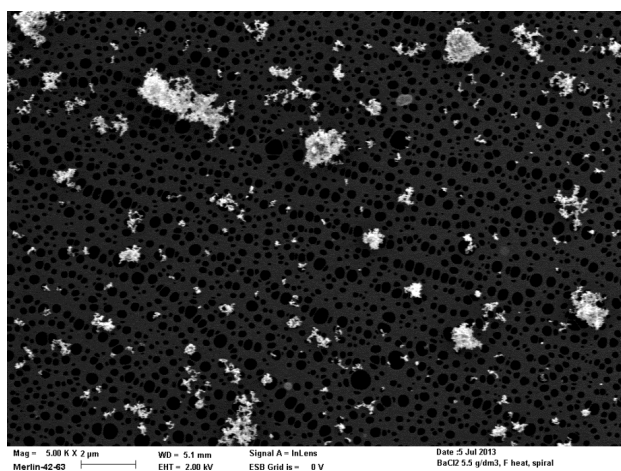


Figure 28a. The generated particles with BaCl_2 (5.5 g/dm^3 , 6 ml/min) with filter, heater and spiral inlet tube (4.7.2013, 10:52). Particles mainly chain-like aggregates up to $2 \mu\text{m}$ in size. This is typical morphology for particles with added silica (e.g. Fig. 11).

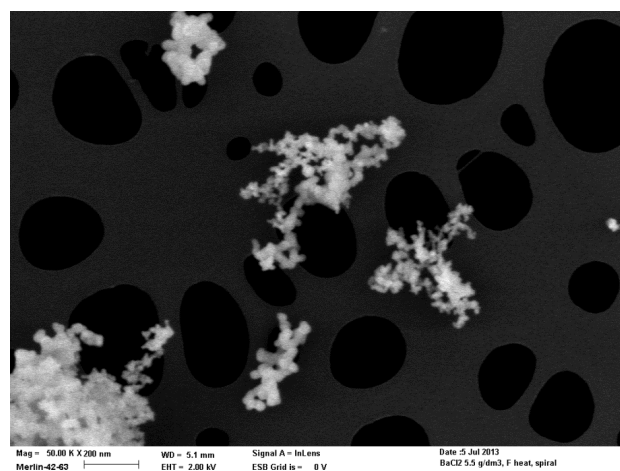


Figure 28b. An image presenting the morphology of 200-300 nm sized aggregates. They consist of almost spherical particles approximately 50 nm in diameter.

4. Summary and conclusions

The IndMeas flow calibrator device (FCD) normally using a cyclone for the collection of produced particles was studied and the produced particles characterised. In this study, though, the cyclone was either removed completely to allow the produced particles directly enter the measurement system (continuous production) or the particles were collected on the surface of a new filter and removed by a fast and powerful “blow” similar as in the case of the cyclone (filter collection).

In the previous experiments particle number and mass concentration and number size distribution has been characterised in detail (Lyyräinen, et al., 2011; Lyyräinen, et al., 2012). In these experiments similar reagents are used to produce the particles as in previous experiments with the exception that the concentration of the feed solutions is further varied and active ^{137}Ba -tracer is applied as in the normal field measurements.

To study the effect of higher temperature on the size of the tracer particles an additional heater ($T=150 \text{ }^\circ\text{C}$; of the same order as temperature at the exit of the FCD) was installed after flow calibration device before the collection filter. The function of the heater is to ensure

that the particles arriving to the filter are completely moisture free that may cause unwanted aggregation/adherence of particles to each other. Moreover, to simulate possible particle adhesion and retention in systems containing moisture near or at the inlet point of the tracer particle feed a so called “wet inlet tube” experiment was carried out. Finally, possible particle adhesion and retention caused by a non-optimal inlet tube was studied by installing a long spiral-type inlet tube.

For **TiO₂ + silica reagent with continuous production** (20 g/dm³, 6 ml/min) the particles were spheres generally larger than 1 μm in diameter. The large spheres consisted of nearly spherical primary particles of approximately 50 nm in size. The size of the spheres was independent of the used reagent concentration.

The produced particles with the **TiO₂ + silica reagent and filter collection** (20 g/dm³, 6 ml/min) were mainly chain-like aggregates. The length of the aggregates varied a lot from a few hundred nanometres up to micrometres. The large spheres seen during continuous production seemed to disintegrate in to smaller chain-like aggregates with filter collection. The disintegration most likely occurs during the powerful pressure “blow” when the collected particles are escaping the filter.

With **Fe(NO₃)₃·9H₂O + silica** reagent with **continuous production** (40 g/dm³, 6 ml/min) the particles were mainly spheres generally larger than 1 μm in diameter as in the case of TiO₂. Decreasing the Fe(NO₃)₃·9H₂O reagent concentration in to 1/20 did not seem to have any significant effect on the size of the agglomerated spheres as in the case for TiO₂. In this case, though, no silica was added. The most probable cause for silica addition type particles is the filter itself: even though the filter was cleaned before and after each experiment the porosity of the filter stores particles from previous experiment that are nearly impossible to remove completely.

With the reference reagent **BaCl₂ with continuous production** (5.5 g/dm³, 6 ml/min) the particles were nearly spheres generally larger than 1 μm as in previous cases (Lyyräinen, et al., 2011 and 2012). However, also smaller, approximately from 0.1 μm to 0.5 μm almost spherical particles were discovered. The structure of the spheres looked highly sintered.

The produced particles with **TiO₂ + silica reagent with filter collection and heater** (20 g/dm³, 6 ml/min) were mainly chain-like aggregates as in the case without heater. Dilution of the reagent concentration in to half did not have any significant effect on the chain-like aggregate or primary particle size (approximately 50 nm).

With **Fe(NO₃)₃·9H₂O + silica** (40 g/dm³, 6 ml/min) reagent with **filter collection and heater** the particles were mainly spheres generally larger than 1 μm in diameter as in the case without the heater. SEM sample for the 1/20 diluted Fe(NO₃)₃·9H₂O reagent was not sampled because the activity of the collected particles was too low. Thus the produced activity signal would have been difficult to filter out from the background noise.

With the reference reagent **BaCl₂** (5.5 g/dm³, 6 ml/min) with **filter collection with heater** the particles were mostly chain-like aggregates up to approximately 1 μm size. The aggregates consisted of small spherical primary particles similar to cases with TiO₂ added silica. Thus it is possible that the sample was contaminated with silica because BaCl₂ particles should like sintered spheres. The most probable cause for silica contamination was the filter itself: even though the filter was cleaned before and after each experiment the porosity of the filter stores particles from previous experiment that are nearly impossible to remove completely.

The produced particles with **TiO₂ + silica reagent** (20 g/dm³, 6 ml/min) **with filter collection, heater and wet inlet tube** were mainly spherical aggregates larger than approximately 1 μm in diameter. This is in contradiction with the case without the wet inlet tube, where the particles were mainly chain-like aggregates. The most probable cause for silica

contamination was the filter itself: even though the filter was cleaned before and after each experiment the porosity of the filter stores particles from previous experiment that are nearly impossible to remove completely. Dilution of in to half did not have any significant effect on the size of the aggregates or primary particle size.

For **Fe(NO₃)₃·9H₂O + silica** (40 g/dm³, 6 ml/min) with **filter collection, heater** and with a **wet inlet tube** the particles were mainly spheres generally larger than 1 μm in diameter as in the case without the wet inlet tube. This indicated that that the wetting of the inlet tube may have been insufficient because basically no trapping of particles had occurred. Therefore, the experiment was repeated, and the size of the penetrated particles was found to be smaller as in the case of ELPI measurement (Fig. 17 at 11:15 vs. 10:35, yellow curve. Decreasing the Fe(NO₃)₃·9H₂O concentration from 40 g/dm³ to 2 g/dm³ caused a clear decrease in the number of the penetrated particles and their size.

For **BaCl₂** (5.5 g/dm³, 6 ml/min) with **filter collection, heater and wet inlet tube** similar structures as without the wet inlet tube were discovered. However, the portion of the almost spherical aggregates generally larger than 1 μm seemed to be higher than without the wet tube. Approximately 3-fold decrease in number concentration compared to the case without the wet tube was found.

The produced particles with **TiO₂ + silica reagent** (10 g/dm³, 6 ml/min) **with filter collection, heater and spiral inlet tube** were mainly chain-like aggregates generally smaller than μm in size. Moreover, the number of the particles was low thus indicating severe trapping by the spiral inlet tube. This was also verified by ELPI measurement where the number concentration decreased nearly 1/20 with the spiral inlet tube. Doubling the reagent concentration increased the number of the penetrated particles to 3.5-7-fold compared to the lower concentration case. In addition, the particles were no longer only chain-like aggregates but also almost spherical particles generally larger than 1 μm in diameter were observed.

For **Fe(NO₃)₃·9H₂O** (2 g/dm³, 6 ml/min) with a **spiral inlet tube and with filter collection and heater** the number of the observed particles was really low, up to two orders of magnitude in total particle number concentration thus indicating severe trapping of the spiral inlet tube. The penetrated particles were of many different shapes. Increasing the reagent concentration to 20-fold and adding **silica** increased then number of the penetrated particles up to 50-fold. The particles were chain-like and spherical aggregates generally larger than 1 μm in diameter.

For **BaCl₂** (5.5 g/dm³, 6 ml/min) with **filter collection, heater and spiral inlet tube** on the particles were chain-like and nearly spherical aggregates generally larger than 1 μm. The most probable cause for the silica contamination is the filter itself: even though it was also cleaned by several pressure “blows” before and after each experiment the porosity of the filter material will store particles from previous experiments that may escape during the following experiment(s). The number of the particles was clearly lower, approximately 2-fold lower than without the spiral tube thus indicating once again the efficient particle trapping of the spiral inlet tube.

As found in the earlier studies with the filter collection the IndMeas flow calibrator device (FCD) is able to produce small particles (<< 1μm). In addition, it seems that the new filter used to collect them causes some agglomeration of the particles into larger ones. However, in the case of TiO₂ + silica with the filter collection the large spheres seen during continuous production seemed to disintegrate in to smaller chain-like aggregates. The disintegration most likely occurs during the powerful pressure “blow” when the collected particles are escaping the filter.

The change of reagent concentration did change the number of produced particles but their size remained basically unchanged. Lowering the reagent concentration even more would

not probably be of any use because collection times (to attain high enough activation level of the particles) would also need to be increased thus increasing the probability for agglomeration on the filter. The addition of additional heaters/insulation on the particle collection line may have some effect.

The addition of an additional heater clearly improved the collection of the particles on the filter by decreasing thermophoretic losses on the walls. The addition of a wet inlet tube to simulate possible particle adhesion and retention in systems containing moisture near or at the inlet point of the tracer particle was found effective in trapping the particles: up to 2.5-fold decrease in number concentration was found. The easiest solution to avoid such trapping would be to make such an inlet probe that could bypass the possible wet spots near actual inlet. However, that is not always possible. Another, even more efficient particle trap was an addition of a long spiral inlet tube to simulate non-optimal inlet tube causing particle adhesion and retention: up to 20-fold decrease in number concentration was found. Thus selecting an optimal inlet tube is very important to minimise particle losses.

The reentrainment of the particles from the filter during the pressure “blow” may be improved by selecting another filter material that is less porous. The main problem in finding a suitable filter material is that it has to withstand the high pressure peak reentraining the particles during the “blow”. One solution could be a dense metal grid or sintered metal filter. These types of filters withstand pressure peaks, and the detachment or reentrainment of the collected particles should be easier.

References

Baltensperger, U., Weingartner, E., Burtscher, H. and Keskinen, J. (2001) Dynamic mass and surface area measurement. In: *Aerosol Measurement – Principles, techniques and applications* (Edited by Baron, P. A. and Willeke, K.). John Wiley and Sons. Pp. 387–418.

Cleen MMEA factsheet (Dec 2010). Measurement, monitoring and environmental assessment – innovations through new thinking. http://www.cleen.fi/home/sites/www.cleen.fi/home/files/Cleen_Factsheet_MMEA_final.pdf.

Keskinen, J., Pietarinen, K. and Lehtimäki, M. (1992) Electrical low-pressure impactor. *J. Aerosol Sci.* 23, 353-360.

Lyyränen, J., Laukkanen, V., Ahlfors, K. and Auvinen, A. (2011) Characterisation of the produced particles by the IndMeas industrial flow calibration device. VTT research report VTT-R-04408-11, 25 p.

Lyyränen, J., Laukkanen, V., Ahlfors, K. and Auvinen, A. (2012) Characterisation of the produced particles by the IndMeas industrial flow calibration device - reagent and filter collection experiments. VTT research report VTT-R-03689-12, 38 p.